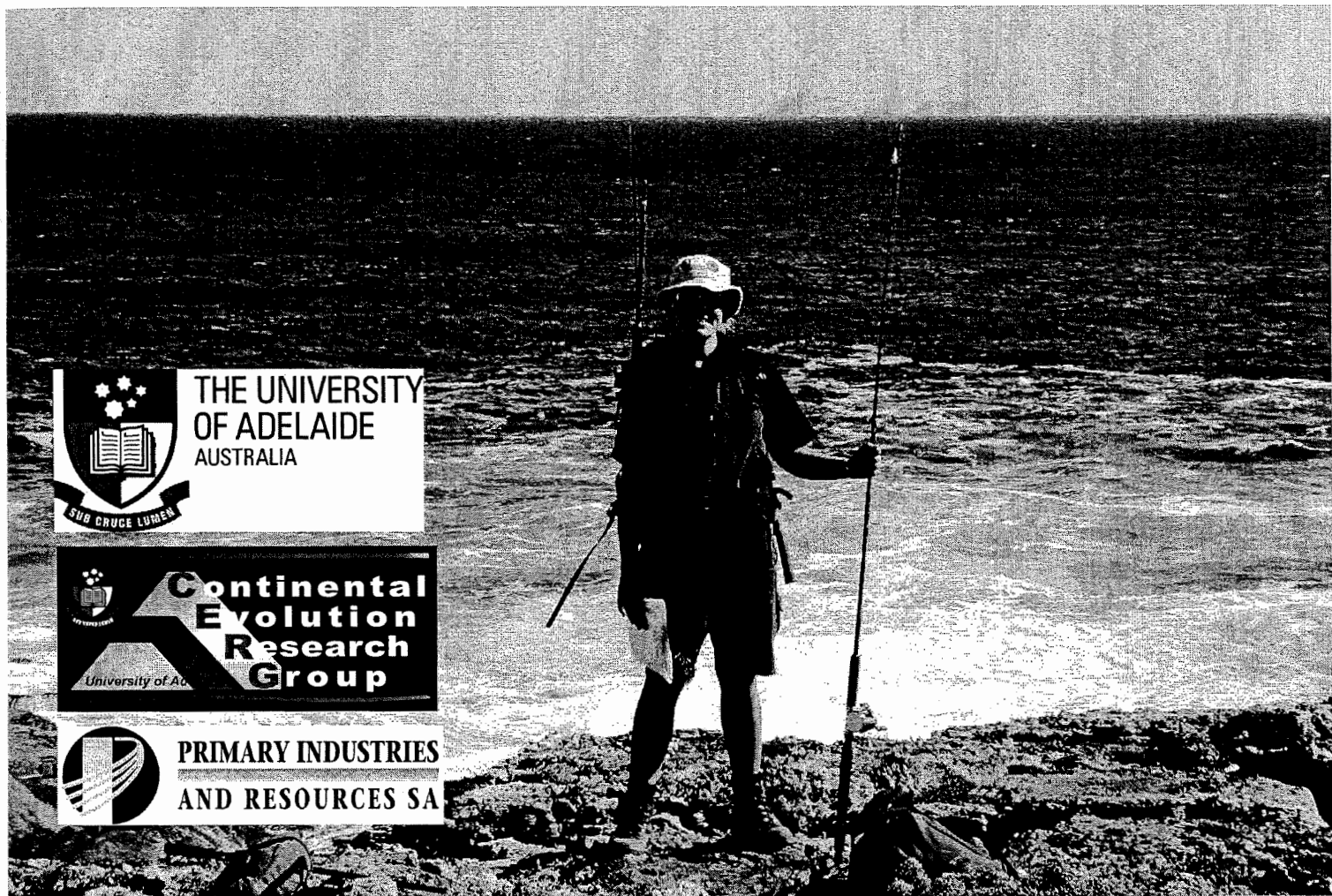


# Provenance of Late Archaean metasedimentary rocks on the southern Gawler Craton: Implications for its early crustal development



Woodhouse, A.J.  
*Geology and Geophysics*  
*School of Earth and Environmental Sciences*  
*The University of Adelaide, Adelaide, Australia*

2002

## Table of Contents

---

List of Figures	3
List of Tables	3
Abstract	4
1. Introduction	5
2. Sampling and analytical methods	7
3. Geological Framework for the Early Gawler Craton	8
3.1 <i>The Southern Gawler Craton</i>	8
4. Results	11
4.1 <i>SHRIMP U-Pb detrital zircon data</i>	11
4.2 <i>Geochemical analyses</i>	13
4.3 <i>Sm-Nd isotopic data</i>	14
5. Interpretation of the geochemistry	15
5.1 <i>Effects of partial melting</i>	15
5.2 <i>Effect on Sm-Nd isotopes</i>	17
6. Discussion	17
6.1 <i>Provenance of Sleaford Complex Metasedimentary Rocks</i>	17
6.1.1 <i>SHRIMP U-Pb detrital zircon ages</i>	17
6.1.2 <i>Constraints on deposition of the Sleaford Complex metasediments</i>	18
6.1.3 <i>Onset of the Sleafordian Orogeny</i>	18
6.1.4 <i>Geochemical constraints on provenance</i>	19
6.1.5 <i>Sm-Nd Isotopes</i>	20
6.2 <i>Hall Bay Volcanics or Volcanoclastics?</i>	21
6.3 <i>Depositional setting for the Sleaford Complex metasediments</i>	22
7. Conclusions	24
8. Acknowledgements	25
9. References	25
Appendix	54

## List of Figures

---

Figure Captions	35
Figure 1.	38
Figure 2.	39
Figure 3.	40
Figure 4.	41
Figure 5.	43
Figure 6.	45
Figure 7.	46
Figure 8.	46
Figure 9.	47
Figure 10.	48
Figure 11.	49
Figure 12.	49
Figure 13.	51

## List of Tables

Table 1.	52
Table 2.	52
Table 3.	53
Table 4.	54
Table 5.	55
Table 6.	56
Table 7.	57

**Provenance of Late Archaean metasedimentary rocks on the southern Gawler Craton:  
Implications for its early crustal development**

Woodhouse, A.J.

*Geology and Geophysics,*

*School of Earth and Environmental Sciences*

*University of Adelaide, Adelaide, Australia*

**Abstract**

Geochemical, whole rock Sm-Nd and detrital zircon U-Pb isotopic data from Archaean metasedimentary successions in the southern Gawler Craton indicate derivation from Late Archaean sources. Detrital zircons from the upper amphibolite-grade Wangary Gneiss have dominant U-Pb age groupings at 2500-2580 Ma and 2600-2720 Ma, with a few analyses ranging up to 2950-3150 Ma. Steep LREE enrichment REE with  $(La/Yb)_N = 46 - 58$  and low abundances of compatible trace elements point to a major felsic source component, with REE patterns typical of Na-rich granites. Detrital zircons from the metasedimentary dominated Hall Bay Volcanics (2500-2560 and 2660-2710 Ma) show a similar range of detrital zircon ages to the Wangary Gneiss, suggesting both sequences were derived from a temporally similar Late Archaean source terrain. The Carnot paragneisses and the Hall Bay Volcanics metasedimentary rocks show comparative HREE enrichment ( $(La/Yb)_N = 7.4-12.5$  and  $(La/Yb)_N = 10.2-15.7$  respectively), suggesting a greater input of mafic or intermediate material relative to the Wangary Gneiss. The correspondence in detrital zircon ages between the Wangary Gneiss and Hall Bay Volcanic metasedimentary rocks suggests both units form part of the same succession. Existing zircon U-Pb data provides no evidence for input of Early Archaean crust into the Wangary Gneiss, Hall Bay Volcanics or Carnot paragneisses, which is further substantiated by Sm-Nd depleted mantle model ages that range from 2900 to 3200 Ma in all metasedimentary rocks. The overlap of detrital zircon and depleted mantle model ages suggests that all three successions in the southern Gawler Craton comprise a single basinal succession. The geochemical compositions of the late Archaean sequences in the southern Gawler Craton are consistent with derivation from a bimodal terrain with variable mixing of three distinct sources: (1) intermediate-felsic volcanics; (2) mafic rocks and (3) highly fractionated Na-rich felsic rocks (tonalites-trondhjemites). These source regions are currently unidentified in the Gawler Craton, however, source terrains for the

*Ailsa Woodhouse, 2002.*

late Archaean sequences may be preserved in association with the 2500-3000 Ma age crust in rifted off components of the Gawler Craton in Antarctica. Although speculative at this stage, deposition of the Late Archaean sequences in the southern Gawler Craton is likely to have occurred on a rifting margin to a Late Archaean terrain. Sedimentation was terminated during collisional closure of the basin system leading to the 2500-2400 Ma Sleafordian Orogeny.

Key Words: Late Archaean, Provenance, Gawler Craton, REE, zircon U-Pb, isotopes.

## **1. Introduction**

Important information about the composition and evolution of Archaean crust and their tectonic setting is recorded in their clastic sedimentary rock record (e.g. Nance and Taylor 1976; McLennan and Taylor 1984; Taylor and McLennan, 1985; Michard et al., 1985; Maas and McCulloch, 1991; Timmerman & Daly, 1995; Toulkeridis, et al., 1999). Previous studies have showed that many Archaean sedimentary sequences have sampled a complex provenance of volcanic, plutonic, metamorphic and sedimentary rocks (e.g. Taylor and McLennan 1985). Despite this complex mix of sources, trace and rare earth elements (REE) are regarded as an accurate discriminator between these variable geochemical provenances (e.g., McLennan and Taylor 1984; Taylor and McLennan 1986; Maas and McCulloch 1991; McLennan et al., 1993; Kalsbeek et al., 1999; Lahtinen et al., 2002). Together, geochemical and Sm-Nd isotopic data from sedimentary rocks are effective approaches in establishing the average isotopic signature of the protolith and its average geochemical composition; however they are ineffective in delimiting contributions from different sources of similar rock types of contrasting ages. In contrast, U-Pb dating of detrital zircons is a non-averaging analytical technique, in that the age of individual components of a source terrain are obtained. Possible zircon-poor mafic rocks are commonly not represented in detrital zircon data sets, but to some extent this problem can be resolved through Sm-Nd isotopic and geochemical compositions of sequences, which are sensitive to a mafic input (e.g. Beakhouse et al. 1999; Lahtinen et al., 2002). In combination, whole rock geochemistry, Sm-Nd isotopic data and U-Pb dating of detrital zircons, produces complementary data sets that allow characterization of the nature of the crust contributing to metasedimentary sequences. These constraints provide a basis for reconstruction of the original crustal elements of the terrain (e.g. Maas & McCulloch, 1991; McLennan et al., 1995; Jahn et al., 1998; Lahtinen et al., 2002).

*Ailsa Woodhouse, 2002.*

This paper presents SHRIMP U-Pb detrital zircons, geochemical and Sm-Nd isotopic data from late Archaean supracrustal components of the southern Gawler Craton, South Australia. This period in the development of the Gawler Cratons is poorly understood, with little work specifically targeted at identifying the sources of sequences and the timing and processes of major phases of crustal growth.

The southern Gawler Craton (Figure 1) has a complex tectonic history (Daly and Fanning, 1993; Fanning 1997; Daly et al, 1998.) and is characterised by poor outcrop, which obscures primary geological relationships. To a large extent this lack of outcrop has hampered the development of tectonic models describing the evolution of the Gawler Craton. However, a recent model proposed by Schwarz et al., (2002) emphasizes the possible role of accretionary style processes during the Palaeoproterozoic, in which the Gawler Archaean domain acted as a cratonic nucleus onto which the younger material was accreted. To further our understanding of the Archaean development of the Gawler Craton two critical questions must be addressed. Firstly do we consider the Gawler Craton Archaean a contiguous domain or a collage of exotic accretionary units? Secondly if it was a contiguous domain what was its composition and what characterised the major events in its crustal evolution? In order to comprehensively address these questions we must initially assess the origin of the Archaean metasedimentary rocks across the Gawler Craton, to characterize the source terranes associated with its early crustal development. There are two main regions of the craton characterised by the presence of Archaean rocks. In the central of the Gawler Craton is the Mulgathing Complex, and in the southern part of the craton the Sleaford Complex (Daly and Fanning, 1993; Daly et al, 1998). This study is focused on the Sleaford Complex.

The main objectives of this study are to:

1. Determine the provenance of the sedimentary-dominated Carnot paragneisses, Hall Bay Volcanics and the Wangary Gneiss, which together comprise the bulk of the Sleaford Complex,
2. To place the deposition of these sequences into a tectonic context.

*Ailsa Woodhouse, 2002.*

We assemble U-Pb isotopic analysis of detrital zircons, Sm-Nd isotopic and geochemical datasets on the metasedimentary rocks of the Sleaford Complex. This study has been undertaken in parallel with Swain (2002) as part of a broader investigation into the late Archaean evolution of the Gawler Craton.

## **2. Sampling and analytical methods**

All samples for this study were obtained from the Sleaford Complex in the southern Gawler Craton (Figure. 2). The complex contains three metasedimentary dominated sequences (Daly and Fanning, 1993; Fanning 1997; Teale et al., 2000). They are;

1. Wangary Gneiss
2. Carnot paragneisses
3. Hall Bay Volcanics

The sampling localities for this study are shown in Figure 2, which also shows sample locations used in previous studies, (Fanning, 1997; Schaefer, 1998; Teale, 2000; Rich, 2000 and M.E.R. data, in prep.). These datasets will be compiled with the data obtained from this study. Note the unpublished data from The Office of Minerals and Energy Resources (M.E.R.) has been provided as an in-kind contribution to this project and has not previously been the focus of detailed analysis.

The analytical techniques for U-Pb detrital zircon analyses are similar to those in Goodge et al., (2001). Zircon separation was done using standard heavy-liquid and magnetic methods followed by hand picking of a representative detrital zircon population sample set. The zircons were mounted on an epoxy disc together with grains from reference zircon. The zircons were sectioned and imaged using optical microscopy and cathodoluminescence (CL) on a scanning electron microscope. 20-30 $\mu$ m areas of both cores and rims that were optically clear, crack free and representative of a single domain in CL images were analysed on SHRIMP I and II at the Research School of Earth Science at the Australian National University, Canberra, under standard operating conditions (Compston et al. 1992; Williams, 1998). Data reduction was done with SQUID 1.02 (Ludwig 2001a) where analyses with >20% discordance were discarded. Weighted mean age calculations were made using Isoplot/Ex 2.49 (Ludwig 2001b).

*Ailsa Woodhouse, 2002.*

Samples for whole rock Sm-Nd isotopes and elemental analyses were crushed in a tungsten-carbide mill. Elemental whole rock analyses were performed at AMDEL Ltd, Adelaide, S.A. Major element analysis as well as Cr, V, Sc and Zr use 0.1 g sub-sample of analytical pulp, which is fused with lithium metaborate followed by dissolution to give a total solution and is presented to an Inductively Coupled Plasma optical emission spectrometer (ICPOES). Rb, Ba, Sr, Hf and Be analyses are determined by presenting the same solution from to an Inductively Coupled Plasma Mass Spectrometer (ICPMS). Lower detection limits for REE, Y, Ni, Co, Cu, Zn, Cs, Tl, Pb, Th, U, Nb, Mo, W, Bi, Ag, As, Pr and Ga are achieved by utilizing a HF/multi acid digest which is presented to an ICPMS. Au, in ppb is analyzed with up to 50 g of sub-sample fused in a lead collection fire assay, the resulting prill is digested in aqua-regia and the gold content of the sample is determined by ICP-OES.

Analytical techniques for whole rock Sm-Nd isotope data have been detailed elsewhere (Foden et al., 1995) and are only summarised here. Sm-Nd isotopic analysis were done at the University of Adelaide. ~0.05 g of whole rock sample powder was spiked with ~0.3 g  $^{150}\text{Nd}$ - $^{147}\text{Sm}$  solution. Sm-Nd samples were digested in HF/HNO<sub>3</sub> in sealed high pressurized teflon bombs for 4 days at 190°C, evaporated in HCL, and sealed again in bombs overnight. The samples were centrifuged for 5 minutes at 13200 rpm then loaded into cation exchange columns for separation. Biorad Poly Prep columns with 2ml AG50W X8 200-400 mesh Biorad cation exchange resin was used for the first stage of Sm-Nd separation, followed by Sm and Nd separation using Sm-Nd columns, which have 2ml of Teflon powder, impregnated with HDEHP.

Sm-Nd concentrations were calculated by isotope dilution and isotope ratios measured by thermal ionization mass spectrometry on a Finnigan MAT-262 mass spectrometer. Reproducibility is tracked by full procedural analyses of an in-house standard, average =  $0.511598 \pm 4$  ( $2\sigma$ ;  $n=23$ ). The average for the La Jolla Nd standard is  $0.511838 \pm 5$  ( $2\sigma$ ). Total blanks for Sm-Nd are 100-200 pg.

### **3. Geological Framework for the Early Gawler Craton**

The Gawler Craton is an extensive crystalline basement province of Archaean to Mesoproterozoic age located in southern Australia (Figure 1). It preserves a complex tectonic history with a number of major tectonic events that variably affected most of the craton (e.g.

*Ailsa Woodhouse, 2002.*

Daly et al., 1998) followed by stabilization *ca* 1450 Ma (Thomson, 1975; Parker, 1993). This study is primarily concerned with the Archaean to early Palaeoproterozoic development of the southern Gawler Craton. This period was marked by the development of the early Palaeoproterozoic (2440-2420 Ma) Sleafordian Orogeny (Fanning 1997; Daly et al., 1998), which strongly affected late Archaean sedimentary and igneous associations across the craton.

Although the Sleafordian Orogeny was identified a number of years ago (e.g. Bradley, 1972; Fanning, 1986; Daly and Fanning 1993; Daly et al., 1998) there are still few detailed descriptions about its metamorphic evolution or the crustal evolution that preceded it. Despite the intensity of deformation and metamorphism associated with the Sleafordian Orogeny a number of pre-Sleafordian lithological units have been identified in the Sleaford Complex. These units define the Late Archaean evolution of the Gawler Craton and are briefly described below.

### *3.1. Southern Gawler Craton-The Sleaford Complex*

The Sleaford Complex (Thompson 1980, Figure) is located on southern Eyre Peninsula (Figure 2). It comprises a complex assemblage of Late-Archaean medium and high-grade metasedimentary sequences, volcanics and granitoids, unconformably overlain by Palaeoproterozoic Hutchison Group metasediments (deposited 2000-1850 Ma; Daly and Fanning, 1993).

#### *3.1.1 The Carnot Gneisses*

The Carnot Gneisses (Figure 2) are a layered sequence of intensely deformed and metamorphosed paragneisses with associated mafic and felsic orthogneisses. Limited Sm-Nd and zircon U-Pb isotopic data (Tables 1 and 2; Fanning, 1997, Schaefer 1998) suggest that the Carnot paragneisses were deposited on as yet unidentified Archaean basement. The Carnot paragneisses are dominated by garnet gneisses that yield preliminary SHRIMP U-Pb zircon ages ranging from 2300-2850 Ma with a few analyses at 2950 to 3150 Ma (Fanning 1997). Ages older than *ca.* 2500 Ma probably represent detrital zircon grains. Medium to coarse-grained concordant bodies of opx-bearing gneiss intruded the Carnot paragneiss supracrustal sequence (Daly and Fanning 1993). The opx-bearing gneiss yields preliminary SHRIMP U-Pb zircon ages from 2600-2500 Ma with a dominant metamorphic peak around 2400 Ma (Fanning 1997). Peak granulite facies metamorphism associated with the Sleafordian Orogeny is recorded by Rb-Sr and U-Pb isotope data to be in the interval *ca* 2400-2440 Ma (Fanning 1997). Mafic dykes or sills that intruded the

*Ailsa Woodhouse, 2002.*

paragneiss sequence at or prior to peak metamorphism are now boudinaged tholeiitic basic granulites (Fanning et al. 1981, Fanning in Parker et al., 1981, Daly and Fanning 1993, Fanning 1997).

### *3.1.2 Wangary Gneiss.*

The Wangary Gneiss consists of amphibolite facies quartzo-feldspathic gneisses that outcrop along the western coastline of the southern Eyre Peninsula (Figure 2), and has been interpreted as a possible lower grade equivalent to the Carnot paragneisses (Daly and Fanning 1993). Preliminary SHRIMP U-Pb zircon analyses (Table 2) yield dominant ca 2480 Ma ages interpreted as a metamorphic age. In addition zircons with an age around  $2679 \pm 9$  Ma has been interpreted as a detrital input into the Wangary Gneiss metasediments, possibly volcanic in origin (Fanning 1997). Sm-Nd isotopic signatures from previous works are shown in Table 1, (Schaefer, 1998; Rich, 2000, M.E.R. data in prep./).

### *3.1.3 Dutton Suite*

The Dutton Suite (Fanning in Parker et al, 1985, Fanning 1997) is an igneous suite relating to a major high crustal level batholith that encompasses the Coultas Granodiorite, the Kiana Granite and the Whidbey Granite (Figure 2; Daly et al., 1998, Daly and Fanning 1993). The Coultas Granodiorite is the oldest member of the suite with a SHRIMP U-Pb intrusive age of  $2517 \pm 14$  Ma (Fanning, 1997). The Kiana Granite has an interpreted SHRIMP U-Pb zircon intrusive age of ca 2460 with significant inheritance around 2550 Ma (Fanning 1997; Table 2). Existing Sm-Nd isotopic data from the Kiana granite indicates significant amounts of assimilated older crust (Iwanwi, 2000). The only radiogenic age data on the Whidbey Granite is a Rb-Sr total rock isochron of  $2337 \pm 71$  Ma (Webb et al, 1986). Outcrop of the Kiana Granite is widespread throughout the western southern Eyre Peninsula where it intrudes the Coultas Granodiorite and the Wangary Gneiss (Daly et al, 1998). The Whidbey Granite outcrops exclusively offshore on islands off the western coast of the southern Eyre Peninsula. It contains enclaves of the Coultas Granodiorite, however relationships between the Kiana Granite and Whidbey Granite are not known (Daly and Fanning 1993).

### *3.1.4 The Hall Bay Volcanics.*

The Hall Bay Volcanics (Figure 2) are a comparatively recently recognised association within the Sleaford Complex and consist of low-grade aluminous and sub-aluminous metapelites

*Ailsa Woodhouse, 2002.*

interlayered with interpreted felsic volcanic and volcanoclastic units (Teale et al., 2000). At present the only known occurrences of the Hall Bay Volcanics are subsurface, located in the Mount Hope area (Figure 2) where they were intersected in drill holes. U-Pb SHRIMP data from two samples of the Hall Bay Volcanics suggest an extrusive age of *ca* 2520 Ma with significant inheritance at 2720 Ma (Teale et al., 2000) due either to the involvement of  $\sim$ 2720 Ma crust in the genesis of the volcanics, or in the provenance of the volcanoclastics.

The relationships between the metasedimentary dominated associations, Carnot paragneisses, Hall Bay Volcanics and the Wangary Gneiss are obscured by comparatively poor outcrop and the affects of mid-Palaeoproterozoic tectonism. However, the Wangary Gneiss and the Hall Bay Volcanics are both low-grade rocks intruded by the Kiana Granite, placing them in a similar temporal position. Their association with the Carnot paragneisses cannot be deciphered through field relationships.

#### **4. Results**

In the following sections isotopic and geochemical data from the Wangary Gneiss, Hall Bay Volcanics and the Carnot paragneiss from the Sleaford Complex are presented. Zircon U-Pb isotopic data is shown in Tables 3 and 5 and Figures 3 and 5, geochemical data is shown in Tables 4 and 6 and Figures 6, 7, 8, 9 and 10, and Sm-Nd isotopic data in Table 7. and Figure 11. Note: the geochemical data for the Hall Bay Volcanics has been provided by the Office of Minerals and Resources of South Australia (M.E.R. data inprep.) as part of the in-kind contribution to this project. An excerpt of this data can be found in Teale et al., (2000); however, no detailed analysis of the data has been published. In the following sections the Hall Bay Volcanic data is discussed in the same context as data collected during this study.

##### *4.1 SHRIMP U-Pb detrital zircon data*

###### *4.1.1 The Wangary Gneiss*

U-Pb isotopic data from detrital zircons in the Wangary Gneiss sample A2030-2 are shown in Table 5. Figure 3a shows the histogram of the detrital age with > 20% discordance, and Th/U ratios versus detrital zircon age are shown in Figure 3b. The zircons are sub-angular to rounded. Internal morphologies (Figure 4) include distinct angular cores and dark C.L. overgrowths, concentric oscillatory zoning and featureless grains. The dominant detrital zircon population

*Ailsa Woodhouse, 2002.*

ranges in age between 2480-2580 Ma. Detrital zircons analyses, 4.1, 5.1, 16.1, 20.1, 24.1, 26.1, 28.1, 33.1, 39.1, 41.1, 44.1 have Th/U ratios less than 0.2 and vary in age from  $2431 \pm 8$  Ma to  $2601 \pm 8$  Ma (Figure 4(a)), with the majority of analyses ranging between  $2482 \pm 6$  Ma to  $2508 \pm 7$  Ma (excludes analyses 4.1 and 16.1). Low Th/U ratios in analyses 4.1, 24.1, 28.1 and 44.1 correspond to dark C.L zircon overgrowths with an angular core, samples 16.1, 20.1, 33.1, 39.1 and 41.1 are mostly elongate featureless zircons and sample 5.1, aged  $2601 \pm 8$  Ma has distinct concentric oscillatory zoning. Other U-Pb detrital zircon ages ranging from  $2477 \pm 12$  Ma to  $2500 \pm 10$  Ma (Figure 4b) are from analyses 7.1, 10.1, 11.1 and 37.1 which are mostly elongate zircons with oscillatory zoning, and Th/U ratios ranging from 0.28 to 1.18. The majority of U-Pb detrital zircon ages in the range  $2511 \pm 9$  to  $2580 \pm 13$  Ma (Figure 4c) correspond to oscillatory-zoned zircons varying from sub-angular/fragmented to rounded with dark C.L. overgrowths. The Th/U ratios of these zircon analyses have a varied distribution from 0.29 to 1.09 with no apparent correlation with spot of analyses and trends in Th/U ratios (Figure 3b).

Older detrital zircon populations have been grouped into populations around 2600-2680 Ma, 2710 Ma and 2980-3120 Ma (Figure 4d). Analyses 4.2, 40.1, 42.1, 23.2 and 45.1 U-Pb ages range from  $2604 \pm 13$  to  $2675 \pm 9$  Ma and Th/U ratios of 0.45-0.87. Analyses 4.2 ( $2604 \pm 13$  Ma) and 42.1 ( $2675 \pm 9$  Ma) correspond to CL light-coloured cores that have dark C.L. overgrowths. In contrast, analyses 45.1 ( $2636 \pm 8$  Ma) and 23.2 ( $2674 \pm 6$  Ma) are comparatively elongate dark C.L zircons with oscillatory zoning. Analyses 9.1 ( $2712 \pm 18$ ) and 18.1 ( $2709 \pm 18$  Ma) both correspond to CL-light-coloured cores, with dark oscillatory-zoned overgrowths and have Th/U ratios of 0.72 and 0.71 respectively. The oldest U-Pb detrital zircon ages are 38.1 ( $2973 \pm 11$  Ma, Th/U = 0.39), 15.1 ( $3016 \pm 13$  Ma, Th/U = 0.33) and 2.2 ( $3126 \pm 11$  Ma, Th/U = 0.84), all three analyses correspond to clear, light C.L. zircon cores with dark C.L. overgrowths.

#### *4.1.2. Hall Bay Volcanics*

U-Pb isotopic data from the Hall Bay Volcanics are shown in Table 3 and weighted mean ages with < 10% discordance are shown in Figure 5. (M.E.R. data in prep.).

The locations of the analysis spots on the analysed grains are not known. Sample R 432969, (Figure 5a) which is from an interpreted tuff layer (M.E.R. data in prep.) shows a range of detrital ages with a significant number of 2500-2560 Ma zircons and older grains in the range 2660-2720

*Ailsa Woodhouse, 2002.*

Ma. A minor mid-Archaean component is represented by analyses at 3130 Ma and 3440 Ma. Sample R 432967 (Figure 5b) has dominant age of *ca* 2530 Ma (Figure 6; M.E.R. data in prep.) and shows inheritance in the range *ca* 2680 –2720 Ma, with additional analyses at 2780 Ma, 3000 Ma and 3080 Ma respectively. The Th/U ratios for zircon analyses corresponding the interpreted magmatic age of 2530 Ma for R 432967 (Figure 5c) range between 0.3 - 0.9, with the majority of ratios ranging from 0.3-0.4. Older zircons ranging in age from 2680 to 3080 Ma have variable Th/U ratios from 0.4 to 0.9.

## *4.2 Geochemical analyses*

### *4.2.1. Major elements compositions*

Major element data for whole rock samples are presented in Table 4 and 6 and Figure 6. With increasing SiO<sub>2</sub> there is a decrease in Al<sub>2</sub>O<sub>3</sub>, Fe<sub>2</sub>O<sub>3</sub>, TiO<sub>2</sub>, MgO and MnO in all metasedimentary successions (Figure 6). In general the range of SiO<sub>2</sub> contents for the Wangary Gneiss samples is comparable to the Hall Bay Volcanics (54 - 70% and 62-76% respectively). The Carnot paragneisses have lower SiO<sub>2</sub> concentrations (47 - 57%). The Wangary Gneisses and the Hall Bay Volcanics are also comparable in Al<sub>2</sub>O<sub>3</sub> (14-17% and 12-21%), Fe<sub>2</sub>O<sub>3</sub> (1-7% and 4-9%), TiO<sub>2</sub> (0.4-0.7% and 0.5-0.8%), MgO (0.2-3.3% and 1.8-3.8%) and MnO (0.01-0.1% and 0.03-0.1%) contents. The Carnot paragneisses have consistently higher Al<sub>2</sub>O<sub>3</sub>, Fe<sub>2</sub>O<sub>3</sub>, TiO<sub>2</sub>, MgO and MnO values compared to the Wangary Gneiss and Hall Bay Volcanics. Only sample A2030-2 from the Wangary Gneiss plots within Carnot paragneiss major elemental ranges. No systematic relationships between the three metasedimentary dominated associations are observed in CaO, Na<sub>2</sub>O or K<sub>2</sub>O concentrations.

### *4.2.2 Trace elements compositions*

Trace element data for whole rock samples is presented in Table 4 and 6 and Figures 7, 8 and 9. Figure 7 shows Carnot paragneisses and Wangary Gneiss normalized to average Archaean mudstone (Taylor and McLennan 1985). Selected compositional ranges for the Carnot paragneiss are Pb = 13-28, Nb = 5-11, Y = 27-35, Ba = 600-700, Nd = 32-24 and Sm = 5.5-6). The exception to this is sample A2030-81 which plots away from the bulk of the Carnot paragneiss samples, being relatively enriched in Pb (62%), Nb (22%) and Y (63%), and depleted in Ba (370%), Nd (20.5%) and Sm (4.5%). Consequently this sample is plotted separately from the trace and REE fields of the other Carnot paragneiss samples. Normalized to the average Archaean mudstone, La, Ce, Pb, Sr, Nd, Hf, Zr and Sm abundances in the Wangary Gneiss and

*Ailsa Woodhouse, 2002.*

Carnot paragneisses follow the same pattern average just above 1. Normalized trace elements Cs, Rb, Ba, Th, U, Nb, Tb and Y show divergence in the trends of the Wangary Gneiss compared to the Carnot paragneisses. When normalized to primordial mantle trace elements of the Hall Bay Volcanics follow similar trends to the Wangary Gneiss (Figure 8).

Figure 9. shows trace elements Cr, Ni, Sc, V, Th, Sr, and Ba against SiO<sub>2</sub> for the Wangary Gneiss, Hall Bay Volcanics and Carnot paragneisses. There is a negative correlation of Cr, Ni, Sc, V and Ba versus SiO<sub>2</sub>. Carnot paragneisses are characterised by higher Cr, Ni, Sc, V and Ba concentrations and lower SiO<sub>2</sub> than the Wangary Gneiss and Hall Bay Volcanics. However, as with the major elements, Wangary Gneiss sample A2030-2 has trace element abundances comparable to the Carnot Gneiss samples in its Cr, Sc and V abundances. Th and Sr against SiO<sub>2</sub> have a minor positive correlation, with significant overlap between the Wangary Gneiss and Carnot paragneisses (Th = 11.5-20 ppm and 9-15 ppm; Sr = 110-250 ppm and 85-160 ppm) excluding sample A2030-81 of the Carnot paragneisses.

#### *4.2.3 Rare Earth Element compositions*

REE data for whole rock samples are presented in Table 6 and chondrite-normalized REE patterns are shown Figure 10. The REE patterns of the Wangary Gneiss samples are steep  $(La/Yb)_N = 46 - 58$ , with relatively steep HREE  $((Gd/Yb)_N = 3.3 - 4.8)$  and negative to positive Eu anomalies of  $Eu/Eu^* = 0.64 - 1.13$ . The REE patterns of the Carnot paragneiss metapelites from Shoal Point (excluding Sample A2030 81) have a shallower REE patterns compared to the Wangary Gneiss, with  $(La/Yb)_N = 10.2-15.7$ , flat HREE with  $(Gd/Yb)_N = 0.92 - 1.23$  and slightly negative Eu anomalies of  $Eu/Eu^* = 0.93-0.96$ . Carnot paragneiss sample A2030 81 has a significantly different REE pattern from the other Carnot samples; it displays LREE depletion relative to HREE resulting in a lower  $(La/Yb)_N$  ratio of 4.2. The Hall Bay Volcanics REE patterns are directly comparable to the Carnot paragneisses with  $(La/Yb)_N = 7.4-12.5$ , flat HREE with  $(Gd/Yb)_N = 0.81-1.2$  and negative to positive Eu anomalies of  $Eu/Eu^* = 0.93-1.25$ .

#### *4.3 Sm-Nd isotopic data*

The Sm-Nd data from this study for the Wangary Gneiss and Carnot paragneisses are presented in Table 7. Sm-Nd data from previous studies on the Wangary Gneiss, Hall Bay Volcanics and Carnot paragneisses (Schaefer 1998, Rich, 2000 and M.E.R. data. in prep.) are shown in Table 4.

*Ailsa Woodhouse, 2002.*

The Wangary Gneiss, Carnot paragneisses and Hall Bay Volcanics are plotted as  $\epsilon_{Nd}$  versus time in Figure 11. All  $^{147}Sm/^{144}Nd$  ratios of the Hall Bay Volcanics, Wangary Gneiss and Carnot paragneisses (excluding A2030-81) fall in the range of 0.10-0.12. The Wangary Gneiss samples  $\epsilon_{Nd}(t)$  ranging from  $-1.3$  to  $-3.4$  and have depleted mantle model ages (Goldstein et. al., 1984) from *ca* 3000 – 3100 Ma. Initial  $\epsilon_{Nd}$  values for the Hall Bay Volcanics range from  $-3.6$  to  $-3.9$  and have depleted mantle model ages (Goldstein et. al., 1984) around *ca* 3100 Ma. The Carnot paragneisses (excluding sample A2030-81) have an  $\epsilon_{Nd}(t)$  range from  $-0.7$  to  $-4.0$  and have depleted mantle model ages (Goldstein et. al., 1984) from *ca* 2900 – 3200 Ma. Sample A2030-81 of the Carnot paragneiss has a  $^{147}Sm/^{144}Nd$  ratio of 0.13,  $\epsilon_{Nd}(t)$  of  $-24.9$  and a depleted mantle model age *ca* 3400 Ma.

## *5. Interpretation of the geochemistry*

### *5.1 Effects of partial melting on trace and REE*

Before considering trace and REE compositions of these metasedimentary units in order to assess the possible variations in geochemical composition of the source terranes for the late Archaean metasedimentary units in the southern Gawler, it is necessary to consider what impact (if any) partial melting during metamorphism may have played in modifying the original sediment compositions. This is a crucial question as there is evidence for partial melting in both the Wangary Gneiss and Carnot paragneisses.

Fluid saturated partial melting in upper amphibolite grade Wangary Gneiss is observed in locally derived leucocratic melts and tourmaline-rich pegmatites cross-cutting the Wangary Gneiss (Rich, 2000). Fluid saturated partial melting is characterised by the generation of small volumes of melt that will be highly concentrated in incompatible trace and REE (e.g. Ayres and Harris, 1997). However, given their small volume, these melts are unlikely to remove sufficient concentrations of trace and REE from the rock system to drastically change the residual rock bulk composition (e.g. Ayres and Harris, 1997; Bea and Montero, 1999). The preservation of largely anhydrous garnet-rich rocks in granulite grade Carnot paragneisses (Bradley, 1972; Fanning et al., 1981; Daly and Fanning, 1993) was likely to be associated with around 30-40% melt extraction (Schnetger, 1994; White et al., 2001) which could have disturbed the trace and REE composition of the residual rock (e.g. Johannes et al., 1995; Chavagnac et al., 1999; Bea and Montero, 1999).

Trace element plots vs SiO<sub>2</sub> (Figure 9.) show that the Carnot paragneisses in comparison with the Wangary Gneiss are enriched in Sc, Ni, Cr and V by a factor of ~2, which could be due to either a significant mafic source contributing the sediments (e.g. Taylor and McLennan, 1985; Beakhouse et al., 1999; Lahtinen, 2000) or an artifact of extensive partial melting that resulted in the enrichment in compatible elements (e.g. Ayres and Harris). Incompatible elements would be highly depleted if sufficient volumes of partial melt extraction had resulted in a shift in the rocks trace element bulk composition (e.g. Chavagnac et al., 1999; Bea and Montero, 1999); however, the Carnot paragneiss abundances of incompatible elements Sr, Th, and Ba significantly overlap with the Wangary Gneisses, which has undergone far less partial melting than the Carnot paragneiss (Daly and Fanning, 1993; Fanning 1997). The similarity in the incompatible element compositions between the Carnot paragneiss and Wangary Gneiss suggests that partial melting has not substantially affected the composition of the Carnot paragneiss.

Factors controlling the REE content of the rocks are different to those controlling the incompatible trace element distribution. Accessory minerals monazite, xenotime, apatite and zircon rarely contain less than 80-90% of the total REE, Th, U, Zr and Y budget of the majority of crustal rocks (Bea, 1996) and as a consequence, the behavior of these accessory phases during partial melting is likely to be the primary control on the redistribution of these elements.

The transition from amphibolite- to granulite-grade rocks is marked by dramatic decreases in the abundance of apatite (e.g. Bea and Montero, 1999), due to the high levels of apatite solubility in peraluminous melts (Pichavant et al., 1992; Wolf and London, 1994). However, the extraction of apatite hosted REE (high in LREE) via melt loss will not necessarily significantly affect the LREE compositions of the residual rock, as the total REE content contained in apatite is several orders of magnitude less than the REE content in monazite, which is also LREE enriched (e.g. Ayres & Harris 1997; Bea and Montero, 1999). Following apatite dissolution, the remaining REE rich phases monazite and xenotime have comparatively low solubility in peraluminous melts (Rapp and Watson, 1986; Montel, 1993; Wolf and London, 1995). Furthermore, the concentration of REE will not necessarily decrease during dissolution of accessory minerals. This is because the loss of monazite into the melt (reducing the modal proportion of monazite) is to a degree compensated by the loss of melt from the system, reducing the overall volume and

*Ailsa Woodhouse, 2002.*

thereby enhancing the proportions of minerals in the contained in the restite (e.g. Johannes et al., 1995; Bea and Montero, 1999; Chavagnac et al., 1999).

## *5.2 Effects on Sm-Nd isotopes*

Possible disequilibrium of Carnot paragneisses Sm-Nd and Nd isotopes during partial melting must also be considered (e.g. Ayres and Harris, 1997; Gao et al., 1999; Chavagnac et al., 2001). If accessory-phase dissolution fractionated the REE abundances, the Sm-Nd isotopic system could also have been modified (e.g. Bea and Montero, 1999; Chavagnac et al., 1999). Increased scatter of  $\epsilon_{Nd}(T)$  values in metasedimentary rocks with low Nd contents (<20 ppm) is interpreted to correspond to the opening of Sm-Nd systems in metamorphic terranes (e.g. Gruau et al., 1996). Importantly, due to mass balance effects, rocks with high Nd contents are less susceptible to possible re-equilibration the Nd poor systems (<20 ppm); as a result the Sm-Nd systematics of Nd-enriched rocks are less likely to be perturbed by metamorphic events (Gruau et al., 1996). The Carnot paragneisses (excluding A2030-81) have Nd concentrations ranging from 31.5 to 34.5 ppm and are therefore less susceptible to disturbance of the Sm-Nd isotopic system during partial melting

## **6. Discussion**

### *6.1. Provenance of Sleaford Complex Metasedimentary Rocks*

#### *6.1.1. SHRIMP U-Pb detrital zircon ages*

The detrital zircon ages recorded in the metasedimentary dominated units in the Sleaford Complex suggest that sediments were sourced from terrains that had undergone major periods of tectonism over the interval ~2500-2720 Ma. Detrital zircon data from the Carnot paragneiss is sparse (e.g. Fanning, 1997), with no detailed information about relative abundances of different aged detrital populations, but existing zircon U-Pb data from the Carnot paragneiss indicate provenance from sources aged *ca* 2500–2850 Ma with a minor input from *ca* 2950 –3150 Ma (Fanning 1997). These detrital zircon components are similar to those in the Wangary Gneiss (2500- 2720 Ma and 2950-3150 Ma, Figure 3) and Hall Bay Volcanics (2500-2560 Ma, 2660-2720 Ma, 3000-3150 Ma, Figure 5.). The overlap in zircon U-Pb age data from the Wangary Gneiss and Hall Bay Volcanics from *ca* 2500 to 2540 Ma and 2680 to 2720 Ma indicates that they have a shared provenance. This similarity in the detrital zircon populations from the

*Ailsa Woodhouse, 2002.*

Sleaford Complex metasedimentary rocks suggests that all three sequences may belong to the same overall basinal system, derived predominantly from 2500-2720 Ma aged terrains.

### *6.1.2 Constraints on deposition of the Sleaford Complex Metasediments*

The lower limits on the deposition of the Carnot paragneisses are metamorphic zircon U-Pb ages corresponding to the Sleafordian Orogeny, which range from *ca* 2400 to 2440 Ma (Fanning, 1997). Similarly, the deposition of the protoliths of the Wangary Gneiss and Hall Bay Volcanics are constrained by the intrusion of the Kiana Granite (*ca* 2460 Ma, Fanning 1997). A metamorphic limit on the deposition of the Wangary Gneiss is U-Pb zircon ages around 2480 Ma, interpreted as metamorphic zircon growth during the Sleafordian Orogeny (Fanning, 1997). This slightly older *ca* 2480 Ma metamorphic age compared to peak granulite conditions at *ca* 2440-2400 in the Carnot paragneisses is attributed to the Wangary Gneiss being situated higher in the crust during the Sleafordian Orogeny (Fanning, 1997). Low Th/U ratios (< 0.2) in detrital zircons have been interpreted as an indicator for metamorphic zircons (e.g. Whitehouse et al, 1999; Nutman et al., 2000). Applying this criteria, Th/U ratios less than 0.2 have been used to discriminate between detrital and metamorphic zircons in the Wangary Gneiss (Figure 4). The majority of zircon analyses with Th/U ratios less than 0.2 correspond to metamorphic zircons that range from  $2482 \pm 6$  Ma to  $2508 \pm 7$  in age and correspond to dark C.L. zircon overgrowths with an angular core, or elongate featureless zircons, which are consistent with metamorphic zircon morphologies (e.g. Hanchar and Miller, 1993; Nutman et al., 2000). Based on the ages of interpreted metamorphic zircon growth in the Wangary Gneiss, and previous studies of the Carnot paragneiss (Fanning, 1997), it appears that high-grade metamorphism during the Sleafordian Orogeny occurred over an interval of *ca* 100 Ma, from *ca* 2400-2500 Ma.

### *6.1.3. Onset of the Sleafordian Orogeny*

On the basis that morphology and composition can be used to discriminate between detrital and metamorphic zircons, grains shown in Figure 4c, whose ages range from  $2511 \pm 9$  to  $2580 \pm 13$  Ma, are interpreted as detrital zircons due to their oscillatory-zoned, sub-angular/fragmented to rounded morphology, dark C.L. overgrowths and Th/U ratios > 0.2. However, it is apparent that the U-Pb data cannot resolve the timing of the onset of Sleafordian-aged metamorphism from the depositional ages of the sediments. The overlap from 2480 to 2520 Ma in the timing of apparent metamorphic zircon growth and age of detrital input suggests that the deposition of these

*Ailsa Woodhouse, 2002.*

metasedimentary dominated successions continued up until the beginning of Sleafordian Orogeny (at least within error of U-Pb zircon analyses). The metamorphic and detrital zircon U-Pb age data suggest that the Sleaford Complex reflect erosion and orogenic reprocessing of continental material *ca* 2500-2720 Ma in age comparatively soon after its formation. This is a common feature in rapidly evolving Precambrian sedimentation systems (Eriksson et al., 1998).

#### *6.1.4 Geochemistry constraints on provenance*

Geochemical compositions potentially provide insights into the average composition of the source terrains. Since major element concentrations in sedimentary rocks are unlikely to provide an accurate representation of the protolith geochemistry due to substantial fractionation of elements during weathering sedimentation and diagenetic processes, emphasis is placed on the trace and REE compositions.

The Wangary Gneiss has steep REE patterns typical of Na-rich granitic rocks (tonalites-trondhjemites; e.g. McLennan and Taylor (1984); Taylor and McLennan (1985); Drummond and Defant, (1990)). The generation of Archaean plutons with steep LREE/HREE patterns has been interpreted as the result of the melting of basaltic crust with garnet-bearing residue (e.g. Gowler et al., 1982; Martin, 1986; Beakhouse and McNutt 1991). The REE pattern of the Wangary Gneiss is the second most frequently occurring REE pattern in sedimentary rocks of the Archaean (Taylor and McLennan, 1985).

On the other hand, the Carnot paragneiss and Hall Bay Volcanics have REE patterns (Figure 10) that are less steep than the Wangary Gneiss pattern. Such a sedimentary rock pattern is comparable to the most common REE signature in Archaean sedimentary rocks (Taylor and McLennan, 1985). The comparatively flat HREE and intermediate LREE in the Carnot paragneiss and Hall Bay Volcanics are commonly interpreted to reflect a mixture of bimodal suites (Figure 12a; e.g. McLennan and Taylor 1985). It is possible to distinguish between bimodal suite provenance from a dominantly intermediate felsic provenance by comparing the abundance of mafic indicator trace elements such as Cr and Ni (e.g. Maas and McCulloch, 1991; Lahtinen, 2000).  $(La/Yb)_N$  versus Cr (Figure 12b) shows that the Carnot paragneiss has higher Cr concentrations than the Wangary Gneiss and Hall Bay Volcanics. In combination with an intermediate  $(La/Yb)_N$  ratio, the trace element data suggests its provenance is probably a mixture of bimodal suites, with a greater input of mafic material relative to the Wangary Gneiss or Hall

*Ailsa Woodhouse, 2002.*

Bay Volcanics. In contrast, the  $(La/Yb)_N$  vs Cr relationships suggests that the Hall Bay Volcanics are largely derived from intermediate-felsic rocks.

Despite the overlap between Hall Bay Volcanics and Wangary Gneiss detrital zircon patterns in the intervals *ca* 2500 to 2540 Ma and 2680 to 2720 Ma, the variation in REE patterns between the two units suggests that the Wangary Gneiss may have received significantly more sedimentary input from a highly fractionated felsic source with depleted HREE typical of Na-rich granitic rocks. Figure 12c illustrates the REE mixing model for end member sources that contributed to the Sleaford metasedimentary rocks based on Figure 12a. The age of this Na-rich felsic source with highly depleted HREE is probably *ca.* 2580-2640 Ma, given the presence of detrital zircons of this age in the Wangary Gneiss, and their absence in the Hall Bay Volcanics.

#### *6.1.5 Sm-Nd isotopes*

The three Sleaford Complex metasedimentary dominated successions have Nd isotopic compositions which describe the average isotopic evolution of a provenance terrain with  $\epsilon_{Nd}(2520 \text{ Ma}) = -0.7$  to  $-4.0$ . Depleted mantle model ages from 2900 to 3200 Ma in combination with U-Pb detrital zircon ages of *ca* 2500-2720 Ma and 2900-3150 Ma, supports the interpretation that the early history of the Gawler Craton was characterised by major phases of crust growth during the Late Archaean. The disparity of 200-300 Ma between the detrital zircon ages and Nd model ages of the Sleaford metasediments is not significant and can be attributed to the variation in estimates of the evolution of the depleted mantle source (Arndt and Goldstein, 1987). Recalculation of the depleted mantle model ages using Michard et al., (1985), results in the Wangary Gneiss  $T_{DM}$  age of 2700-2800, Carnot paragneisses  $T_{DM}$  ages of 2600-2900 and Hall Bay Volcanics  $T_{DM}$  ages of 2800 having ages considerably closer to the ages their detrital zircon analyses demonstrates how depleted mantle model estimates depend significantly on which model is used. However despite this, depleted mantle model ages for the Hall Bay volcanics, when recalculated with model of Michard et al, (1985), are still considerably older than the dominant zircon ages of 2500-2560 Ma and 2680-2720 Ma. This disparity indicates incorporation of older crust into the Hall Bay Volcanics.

The apparently greater input of mafic material into the protoliths of the Carnot paragneisses is likely to be under represented in its U-Pb detrital zircon analyses, since mafic rocks generally contain few zircons compared to felsic rocks. The depleted mantle model ages ranging from *ca*

*Ailsa Woodhouse, 2002.*

2900 to 3200 Ma, when compared with U-Pb detrital zircon ages ranging from 2500 to 2850 Ma and 2900-3150 Ma indicates that inputs of significantly older zircon-free mafic units are not present.

### *6.2. Hall Bay Volcanics or Volcanoclastics?*

The Hall Bay Volcanics have significantly evolved initial  $\epsilon_{\text{Nd}}$  signatures (-3.9 and -3.6) compared to the majority of Late Archaean felsic volcanics (e.g. Henry et al., 2000; Hollings and Wyman, 1999; McCulloch and Bennett, 1994). The combination of these evolved  $\epsilon_{\text{Nd}}$  signatures and the age difference between their depleted mantle model ages and dominant zircon analyses, requires a component of older, more evolved Archaean material.

The nature of the Hall Bay Volcanics has direct implications for the interpretation of the provenance data from the Wangary Gneiss and Carnot paragneisses. There are several lines of evidence that suggest the Hall Bay Volcanics are volcanoclastic/metasedimentary rocks which form part of the same lithostratigraphic sequence as the Wangary Gneiss.

1. The Hall Bay Volcanics are a heterogeneous lithological package, containing interlayered, black pyritic (meta)pelitic rocks, calcsilicates, dolomites and amphibolites (Teale et al., 2000). Despite their low metamorphic grade they preserve no lithologies that could be directly attributed to volcanism (e.g. Winter, 2001). The only substantive evidence for volcanic-derived material is the presence of embayed quartz grains in some units (Teale et al., 2000).
2. Detrital zircons from the Wangary Gneiss and Hall Bay Volcanics have common ages at *ca* 2500-2540 Ma and 2680-2720 Ma (Figures 3 and 5).
3. The initial  $\epsilon_{\text{Nd}}$  signatures of the Hall Bay Volcanics and the Wangary Gneiss are similarly evolved.
4. Both units are intruded by the Kiana Granite.
5. The Hall Bay Volcanics and the Wangary Gneiss are spatially close (Figure 2).

The data suggests that the Hall Bay Volcanics are not representative of a discrete volcanic sequence, but are more accurately a sequence of shallow marine sediments that contain volcanoclastics units, which are indicated by the presence of embayed quartz grains. The source

*Ailsa Woodhouse, 2002.*

for the volcanoclastics are likely to be intermediate felsic volcanics, as represented in the dominant zircon analyses around 2500-2530 Ma (Figure 5 and Teale et al., 2000).

### *6.3 Depositional setting for the Sleaford Complex metasediments*

The simplest view for the depositional environment of the three metasedimentary dominated associations the Hall Bay Volcanics, Wangary Gneiss and Carnot paragneisses, is that all three units were deposited as a part of one extensive basin succession that formed around *ca* 2500-2550 Ma ago. This model is not based on direct stratigraphic correlation, as there are no constraints on sequencing of the stratigraphy, but instead relies on the geochronological and geochemical arguments as presented above.

An obvious question that arises is what was the composition and age of the basement onto which the Sleaford Complex metasediments were deposited? The oldest known igneous rocks within the Sleaford Complex occur within the Hall Bay Volcanics, which have an interpreted magmatic input around 2500-2530 Ma. The majority of SHRIMP U-Pb detrital zircon ages of all of the metasedimentary dominated associations in the Sleaford Complex, range from *ca* 2500 to 2850 Ma, with depleted mantle model ages ranging from 2900 to 3200 Ma. All exposed Archaean cratons are dominated by two lithological associations: (1) tonalite-trondjemite-granodiorite assemblages (TTG-suites) and (2) mafic to intermediate volcanic and sedimentary associations (greenstone belts) (Taylor and McLennan, 1985; Choukroune et al., 1997). The geochemical signature of these lithological associations corresponds to the interpreted sources of the Wangary Gneiss, Carnot paragneisses and Hall Bay Volcanics protoliths. This suggests that the Sleaford Complex metasediments were deposited on an as yet unidentified, late Archaean (2900-2500 Ma) terrain, consisting of an amalgamation of bimodal suites and intermediate felsic volcanics/granitoids. Detrital zircons with Early to Mid Archaean ages ranging from 2950 to 3400 Ma are rare in the Sleaford metasedimentary rocks, with one to three concordant analyses per metasedimentary sample (N = 40-60). Given the paucity of these aged zircons, it is likely that they represent multi cycle components within the 2900-2500 Ma source regions rather than any substantial Early Archaean cratonic material.

Although there are obvious limits to the application of modern day crustal growth processes to explain the evolution of Archaean systems, processes comparable to modern plate tectonic processes such as lateral accretion and continental rift-drift processes have been recognised in

*Ailsa Woodhouse, 2002.*

Late Archaean terranes (e.g. Barley et al., 1998; Wyman 1999; Polat and Kerrich, 2001). Viewed in the context of modern plate tectonic-style processes, a speculative tectonic setting is proposed for the deposition of the protoliths to the Sleaford metasediments. In this model a basin developed along a rifting margin composed of *ca.* 2900-2500 Ma crust consisting of bimodal and intermediate igneous rocks (Figure 13). Rifting associated with the initial development of the passive margin may have generated mafic melts, which may have either undergone intracrustal differentiation, or promoted melting of the thinned 3000-2500 Ma crust, resulting in felsic volcanism. These felsic melts may be represented by the volcanic components of the Hall Bay Volcanics. These mafic melts may also account for the pre-Sleafordian Orogeny mafic rocks within the Carnot paragneisses (Daly et al., 1998). Sedimentation is envisaged to have continued up until *ca.* 2500 Ma, when it was terminated by the onset of convergent deformation, which culminated in the development of the Sleafordian Orogeny (2400-2500 Ma). The period leading up to the onset of the Sleafordian Orogeny was also associated with the generation of the Dutton Suite granites, which in part are the products of major intracrustal differentiation (Iwanwi, 2000). The generation of granites immediately prior to the Sleafordian Orogeny (Coultas Granodiorite), indicates a tectonic setting associated with elevated heat flows, consistent with an evolving rifted margin. Following the Sleafordian Orogeny, there was an interval of  $\sim$  400-500 Ma during which there was little tectonic activity (Daly et al., 1998). This suggests that the system had become temporarily cratonised, and converted into a continental interior. Such a scenario would be most easily achieved if the Sleafordian Orogeny involved collision and amalgamation of continental blocks.

Recent work has highlighted similarities between the southern Gawler Craton and parts of the Antarctic Shield within Terre Adelie and George V Land during their Archaean to Palaeoproterozoic histories (Bennett and Fanning 1993; Fanning and Oliver 1994; Fanning et al., 1996; Oliver and Fanning, 1998; Peucat et al., 1999; Goodge et al., 2001; Fanning et al., 2002). These similarities have been used as a basis to show that large parts of the Antarctic Shield represent the extension of the Gawler Craton (Oliver and Fanning, 1998; Goodge et al., 2001; Fanning et al., 2002). Within this Archaean domain are regions characterized by 3000-2500 Ma rocks with a range of compositions (Goodge et al., 2001) which could have conceivably provided a source for the protoliths of the Sleaford Complex metasediments. In the context of the tectonic setting suggested above, these 3000-2500 Ma rocks would have comprised the protocraton that hosted the rifted margin. Alternatively the Sleaford Complex metasediments may have been

*Ailsa Woodhouse, 2002.*

deposited on a rifting margin linked to an unidentified protocraton before it became an addition to the Antarctic Shield/Gawler Craton during a Palaeoproterozoic collision that may be recorded by the 2400-2500 Sleafordian Orogeny.

## **7. Conclusions**

Geochemical, whole rock Sm-Nd and detrital zircon U-Pb isotopic data from Archaean metasedimentary successions in the southern Gawler Craton indicate derivation from predominantly Late Archaean bimodal sources. Two major crustal province ages emerge from overlapping SHRIMP U-Pb detrital zircon patterns between the Wangary Gneiss, Hall Bay Volcanics and Carnot paragneisses, one around 2500-2560 Ma and one from about 2660-2720 Ma. Early Archaean zircons are rare, emphasizing the dominance of a Late Archaean source terrain. Nd depleted mantle model ages which range from 2900 to 3200 Ma, support late Archaean sources. Contrasting geochemical abundances between the Wangary Gneiss, Hall Bay Volcanics and Carnot paragneisses indicate varying amounts of mafic and felsic sources of bimodal suites contributing to the sequences. The provenances of these Archaean metasedimentary rocks can be summarised as follows:

The Hall Bay Volcanics, which have been reinterpreted as a volcanoclastic sequence, are predominately derived from intermediate-felsic volcanics (*ca* 2500-2530 Ma), and appear to be contemporaneous with deposition of the precursors to the Wangary Gneiss. Detrital zircon data provide evidence of older crustal input around 2660-2720 Ma.

Two distinct protoliths of the Wangary Gneiss have been identified; (a) 2500-2530 Ma intermediate-felsic volcanoclastic input which is probably identical to that in the Hall Bay Volcanics metasediments zircon analyses, (b) a highly fractionated felsic end member, with steep, highly depleted HREE patterns, typical of Na-rich igneous rocks, estimated to be *ca* 2580-2640 Ma in age. The Wangary Gneiss also received an older crustal input around 2680-2710 Ma. The Carnot paragneiss is comparable to typical Archaean mudstones (Taylor and McLennan, 1985), where source terrains are; a mafic source revealed by the unfractionated, flat overall HREE pattern and higher Cr, Ni and Sc abundances, (b) a felsic end member which is indicated by LREE enrichment. Compared to the Wangary Gneiss and the Hall Bay Volcanics the Carnot paragneiss received a greater modal proportion of mafic material

The Sleaford metasedimentary rocks may have been deposited on a rifting margin that developed on a ca. 3000-2500 Ma protocraton composed of bimodal and intermediate igneous rocks that had undergone rapid crustal development. Basin development occurred roughly in the interval 2550 – 2500 Ma and was terminated by the onset of the 2500-2400 Ma Sleafordian Orogeny. This event led to the development of an early Palaeoproterozoic protocraton that was tectonically stable for around 300-400 Ma.

## **8. Acknowledgements**

Thank you Martin Hand for your encouragement and support this year, not to mention your inexhaustible passion for geology, which has always provided me with inspiration. Thank you Karin Barovich for your weekends spent on the mass spec, your cheerful smile and the insight you have given me into the world of geochemistry. I would also like to thank Martin and Karin together, as they are the backbones of CERG and I feel privileged to have had the opportunity to work with such a dynamic, stimulating research group. Thanks to Mike Schwarz and the Gawler Craton team at the Office of Mineral and Energy Resources for helping in the development of my understanding of Gawler Craton Geology and more importantly for the financial support for this project. I would also like to acknowledge Mark Fanning and his help with the analytical work on the SHRIMP.

## **9. References**

Arndt, N.T., & Goldstein S.L., 1987. Use and abuse of crust formation ages. *Geology*, v 15, p 893-895.

Ayre, J.A. and Davis, D.W. 1997, NeoArchean evolution of differing convergent margin assemblages in the Wabigoon Subprovince: geochemical and geochronological evidence from the Lake of the Woods greenstone belt, Superior Provenance, Northwestern Ontario. *Precambrian Research*. 81, 155-178.

Ayres, M. and Harris. N. 1997. REE fractionation and Nd-isotope disequilibrium during crustal anatexis: constraints from Himalayan leucogranites. *Chemical Geology*. 139, 249-269.

Barley, M. E., Krapez, B., Groves, D. I. & Kerrich, R. 1998. The Late Archaean bonanza: metallogenic and environmental consequences of the interaction between mantle plumes, lithospheric tectonics and global cyclicity. *Precambrian Research*. 91, 65-90.

Bea, F. 1996. Residence of REE, Y, Th and U in granites and crustal protoliths: Implications for the chemistry of crustal melts. *J. Petrol.* 37, 521-552.

Bea, F., Montero, P. Garuti, G. & Zacharini, F. 1997. Pressure-dependence of rare earth element distribution in amphibolite- and granulite-grade garnets; a LA-IC-MS study. *Geostandards Newsletter*. 21; 2. 253-270.

Bea, F. & Montero, P. 1999. Behavior of accessory phases and redistribution of Zr, REE, Y, Th, and U during metamorphism and partial melting of metapelites in the lower crust: An example from the Kinzigite Formation of Ivrea-Verbano, NW Italy. *Geochim. Cosmochim. Acta*, 63, No, 1133-1153.

Beakhouse, G.P., McNutt, R.H., 1991. Contrasting types of Late Archean plutonic rocks in northwestern Ontario: implications for crustal evolution in the Superior Province. *Precambrian Research*. 49, 141-165.

Bennett, V.C. & Fanning, C.M. 1993. A glimpse of the cryptic Gondwana shield; Archean and Proterozoic ages from the central Transantarctic Mountains. In *Geological Society of America, 1993 annual meeting*. 25; p 49.

Bradley, G.M., 1972. The geochemistry of a medium pressure granulite terrain at southern Eyre Peninsula, Australia. Australian National University (Canberra). Ph.D. thesis (unpub.).

Chavagnac, V., Nager, T.F. & Kramers, J.D. 1999. Migmatization by metamorphic segregation at subsolidus conditions: implications for Nd-Pb isotope exchange. *Lithos*, 46, 275-298.

*Ailsa Woodhouse, 2002.*

Chavagnac, V., Kramers, J.D., Nager, T.F., Holzer, L., 2001. The behaviour of Nd and Pb isotopes during 2.0 Ga migmatization in Paragneisses of the Central Zone of the Limpopo Belt (South Africa and Botswana). *Precam. Res.* 112, 51-86.

Choukroune, P., Ludden, Chardon, D., Calvert, A.J. and Bouhalliet, H. 1997. Archaean crustal growth and tectonic processes: a comparison of the Superior Province, Canada and the Dharwar Craton, India. In: Burg, J. P. Ford, M. (eds), *Orogeny Through Time*, Geological Society Special Publications No. 121, 63-98.

Compston, W., Williams, I.S., Kirschvink, J.L., Zhang, Z., Ma, G., 1992. Zircon U-Pb ages for the Early Cambrian time-scale. *J. of the Geological Society of London.* 149, 171-184.

Daly, S.J. and Fanning, C.M. 1993. Archaean. In: Drexel, J.F., Preiss, W.V. and Parker, A.J. (editors), *The geology of South Australia. Vol. 1, The Precambrian.* Geological Survey of South Australia, Bulletin 54.

Daly, S.J., Fanning, C.M. & Fairclough, M.C., 1998. Tectonic evolution and exploration potential of the Gawler Craton, South Australia. *AGSO Journal of Australian Geology and Geophysics,* 17, 145-168.

Drummond, M.S., Defant, M.J., 1990. A model for trondhjemite-tonalite-dacite genesis and crustal growth via slab melting: Archean to modern comparisons. *Journal of Geophysical Research,* 95, 21503-21521.

Eriksson, P.G., Condie, K.C., Tirsgaard, H., Mueller, W.U., Altermann, W., Miall, A.D., Aspler, L.B., Catuneanu, O., Chiarenzelli, J.R. 1998. Precambrian clastic sedimentation systems. *Sedimentary Geology.* 120, 5-53.

Fanning, C.M. 1997. Geochronological synthesis of Southern Australia. Part II. The Gawler Craton. South Australia Department of Mines and Energy, Open file envelope 8918 (unpublished).

*Ailsa Woodhouse, 2002.*

Fanning, C.M., Menot, R.P., Peucat, J.J & Pelletier, A. 2002. A closer examination of the direct links between southern Australia and Terre Adelie and George V Land, Antarctica. In: 16<sup>th</sup> Australian Geological Convention, Adelaide, 2002. Geological Society of Australia, Abstracts, 67, p224.

Fanning, C.M., Moore D.H., Bennett, V.C. & Daly S.J. 1996. The “Mawson Continent”; Archean to Proterozoic crust in the East Antarctic Shield and Gawler Craton, Australia; a cornerstone in Rodinia and Gondwanaland. In Geoscience for the community; 13<sup>th</sup> Australian geological convention, 41, 135.

Fanning, C.M. & Oliver, R.L. 1994. Australia and Antarctica reunited; a unique lithological, chemical and isotopic correlation of the Gawler Craton, South Australia and George V Land, Antarctica. In: Geological society of America, 1994 Annual meeting. 26; p504.

Fanning, C.M., Flint, R.B., Parker, A.J., Ludwig, K.R. and Blissett, A.H., 1988. Refined Proterozoic evolution of the Gawler Craton, South Australia, through U-Pb zircon geochronology. *Precam. Res.* 40/41, 363-386.

Fanning, C.M., Oliver, R.L., Cooper, J. A. and Ludwig, K.R., 1986. Rb-Sr and U-Pb geochronology of the Carnot Gneisses: complex isotopic systematics for the Late Archean to Early Proterozoic Sleaford Complex, southern Eyre Peninsula, South Australia. In: 8<sup>th</sup> Australian Geological Convention, Adelaide, 1986. Geological Society of Australia, Abstracts, 15, 69-70.

Fanning, C.M. Oliver, R.L. and Cooper, J.A., 1981. The Carnot Gneisses, southern Eyre Peninsula. South Australian Geological Survey. Quarterly Geological notes, 80:7-12.

Foden, J., Mawby, J., Kelley, S., Turner, S., Bruce, D., 1995. Metamorphic events in the eastern Arunta Inlier, part 2. Nd-Sr-Ar isotopic constraints. *Precam. Res.* 71, 207-227.

Gao, S., Ling, W., Qiu, Y., Lian, Z., Hartmann, G. and Simon, K. 1999. Contrasting geochemical and Sm-Nd isotope compositions of Archean metasediments from the Kongling high-grade terrain of the Yangtze craton: Evidence for cratonic evolution and redistribution of REE during crustal anatexis. *Geochimica et Cosmochimica Acta*, 63 (13/14), 2017-2088.

Goldstein, S.L., O’Nions, R.K. and Hamilton, P.J., 1984, A Sm-Nd study of atmospheric dusts and particulates from major river systems. *Earth Planet Sci. Lett.*, 70, 221-236.

Goodge, J.W., Fanning, C.M. & Bennett, V.C. 2001. U-Pb evidence of ~1.7 Ga crustal tectonism during the Nimrod Orogeny in the Transantarctic Mountains, Antarctica: Implications for Proterozoic plate reconstruction. *Precambrian Research*, 112, 261-288.

Gruau, G., Rosing, M. Bridgwater, D. & Gill, R. C. O. 1996. Restting of Sm-Nd systematics during metamorphism of >3.7 Ga rock: implication from isotopic models of early Earth differentiation. *Chemical Geology*. 133, 225-240.

Hanchar, J.M. Miller, C.F. 1993. Zircon zonation patterns as revealed by cathodoluminescence and backscattered electron images: implication for interpretation of complex crustal histories. *Chemical Geology*. 110, 1-13.

Henry, P. Stevenson, R.K., Larbi, Y.& Garipey, C. 2000. Nd isotopic evidence for Early to Late Archean (3.4-2.7 Ga) crustal growth in the Western Superior Provenance (Ontario, Canada). *Tectonophysics* 322, 135-151.

Hollings, P. and Wyman, D. 1999. Trace element and Sm-Nd systematics of volcanic and intrusive rocks from the Lumby Lake Greenstone belt, Superior Province: evidence for a plume-arc interaction. *Lithos*, 46, 189-213.

Iwaniw, A., 2000. Evidence of recycling of Archaean continental crust; a geochemical and Nd-Sr isotope study of Gawler Craton Granitoids, South Australia. Honours Thesis, Department of geology and geophysics, The University of Adelaide, South Australia, Australia

Jahn, B.M., Gruau, G., Capdevila, R. Cornichet., Nemchin, A., Pidgeon, R. & Rudnik., V.A. 1998. Archaean crustal evolution of the Aldan Shield, Siberia: geochemical and isotopic constraints. *Precambrian Research*. 91, 333-363.

*Ailsa Woodhouse, 2002.*

Johannes, W., Holtz, F. and Möller, P. 1995. REE distribution in some layered migmatites: constraints on their petrogenesis. *Lithos.* 35, 139-152.

Kalsbeek, F., Pulvertaft, T.C.R. & Nutman, A.P. 1999. Geochemistry, age and origin of metagreywackes from the Palaeoproterozoic Karrat Group, Rinkian Belt, West Greenland. *Precambrian Research.* 91, 383-399.

Lahtinen, R. 2000. Archaean-Proterozoic transition: geochemistry, provenance and tectonic setting of metasedimentary rocks in central Fennoscandian Shield, Finland. *Precambrian Research,* 104, 147-174.

Lahtinen, R., Huhma, H & Kousa, J. 2002. Contrasting source components of the Paleoproterozoic Svecofennian metasediments: Detrital zircon U-Pb, Sm-Nd and geochemical data. *Precambrian Res.* 116, 81-109.

Lanzirotti, A. and Hanson, G.N. 1996. Geochronology and geochemistry of multiple generations of monazite from the Wepawaug Schist, Connecticut, USA: Implications for monazite stability in metamorphic rocks. *Contrib. Mineral. Petrol.* 125, 332-340.

Ludwig, K.R., 2001a. Squid 1.02 A users manual. Berkeley Geochronology Center, Berkeley, CA, special Publication No.2

Ludwig, K.R., 2001b. Users manual for Isoplot/Ex, Version 2.49, A geochronological toolkit for Microsoft Excel. Berkeley Geochronology Center, Berkeley, CA, special Publication No.1a

Maas, R. & McCulloch, M.T. 1991. The provenance of Archean clastic metasediments in the Narryer Gneiss Complex, Western Australia: Trace element geochemistry, Nd isotopes and U-Pb ages for detrital zircons.

Martin, H. 1986. Effect steeper Archean geothermal gradient on geochemistry of subduction-zone magmas. *Geology,* v 14, p 753-756, September 1986.

*Ailsa Woodhouse, 2002.*

M.E.R. data in prep. Office of Minerals and Energy Resources, Department of Primary Industries and Resources of South Australia.

McCulloch, M. T. and Bennett, V.C., 1994. Progressive growth of the Earths continental crust and depleted mantle: Geochemical constraints. *Geochimica et Cosmochimica Acta*. 58, 4717-4738.

McLennan, S.M. & Taylor S.R. 1984, Archaean Sedimentary rocks and their relation to the composition of the Archaean Continental crust. In: *Archaean Geochemistry; the origin and evolution of the Archaean continental crust*. Editors; Kroener, A., Hanson, G.N. & Goodwin, A.M. PB Springer-Verlag, Berlin; New York, 1984.

McLennan, S.M., Hemming, S., McDaniel, D.K. & Hanson, G.N. 1993. Geochemical approaches to sedimentation, provenance and tectonics. *Geological society of America. Special Paper 284*, 21-40.

McLennan, S.M., Hemming, S.R., Taylor, S.R. & Eriksson, K.A. 1995. Early Proterozoic crustal evolution: Geochemical and Nd-Pb isotopic evidence from metasedimentary rocks, southwestern North America. *Geochimica et Cosmochimica Acta*. 59, 1153-1177.

Michard, A., Gurriet, P., Soudant, M., Albarede, 1985. Nd isotopes in French Phanerozoic shales: external vs. internal aspects of crustal evolution. *Geochimica et Cosmochimica Acta*, 49, 601-610.

Montel. J.M. 1993. A model for monazite/melt equilibrium and the application to the generation of granitic magmas. *Chem. Geol.* 110, 127-146.

Nance, W.B. & Taylor, S.R., 1976. Rare-earth element patterns and crustal evolution I: Australian post-Archaean sedimentary rocks. *Geochim Cosmochim Acta*, 40, 1539-1551.

Nutman, A. P., Bennett. V.C., Friend, C. R. L., McGregor, V.R. 2000. The early Archaean Itsaq Gneiss Complex of southern West Greenland: The importance of field observations in interpreting age and isotopic constraints for early terrestrial evolution. *Geochim. Cosmochim. Acta*. 64, 3035-3060.

Oliver, R.L. & Fanning, C.M. 1998. George V Land-Adelie Land-Eyre Peninsula; a tentative correlation. In: Geoscience for the new millennium; abstracts. 14<sup>th</sup> Australian Geological Convention, Townsville, 1998. Geological Society of Australia, Abstracts, 49, p341.

O’Nions, R.K., Hamilton, P.J., Hooker, P.J. 1983. A Nd isotopes investigation of sediments related to crustal development in the British Isles. *Earth Planet Science Letters*. 63, 229-240.

Parker, A.J., 1993. Geological Framework. In: Drexel, J.F., Preiss, W.V. & Parker, A.J., (editors), *The Geology of South Australia*. Vol. 1, The Precambrian. Geological Survey of South Australia, Bulletin 54.

Parker, A.J., Fanning, C.M., Flint, R.B., Martin, A.R. and Rankin, L.R, 1988. Archaean-Early Proterozoic granitoids, metasediments and mylonites of southern Eyre Peninsula, South Australia. Geological Society of Australia. Specialist Group in Tectonics and Structural Geology. Field Guide Series, 2.

Parker, A.J., Fanning, C.M. and Flint, R.B., 1985. Geology. In: Twidale, C.R., Tyler, M.J. and Davies, M. (Eds), *Natural History of Eyre Peninsula*. Royal Society of South Australia. Occasional Publications, 4, 21-45.

Peucat, J.J., Ménot, R.P., Monnier, O. & Fanning, C.M. 1999. The Terre Adélie basement in the East-Antarctica Shield: geological and isotopic evidence for a major 1.7 Ga thermal event; comparison with the Gawler Craton in South Australia. *Precambrian Research*, 94, 205-224.

Pichavant, M., Montel, J.M. and Richard, L.R. 1992. Apatite solubility in peraluminous liquids: Experimental data and an extension of the Harrison-Watson model. *Geochim. Cosmochim. Acta*. 56, 3855-3861.

Polat, A. and Kerrich, R. 2001. Geodynamic processes, continental growth, and mantle evolution recorded in late Archean greenstone belts of the southern Superior Province, Canada. *Precambrian Research*, 112, 5-25.

*Ailsa Woodhouse, 2002.*

Rapp, R.P. and Watson, E.B. 1986. Monazite solubility and dissolution kinetics: implications for the thorium and light rare earth chemistry of felsic magmas. *Contrib. Mineral. Petrol.* 94, 304-316.

Rich, B. 2000. An Investigation of the Archaean Wangary Gneiss and its relevance to the evolution of the southern Gawler Craton. Honours Thesis, Department of Geology and Geophysics, The University of Adelaide, South Australia, Australia.

Schaefer, B. 1998. Insights into Proterozoic Tectonics from the southern Eyre Peninsula, South Australia. PhD thesis, Department of Geology and Geophysics, The University of Adelaide, South Australia, Australia.

Schnetger, B. 1994. Partial melting during the evolution of the amphibolite- to granulite-facies gneisses of the Ivrea Zone, northern Italy. *Chemical Geology.* 113; 1-2, p 71-101.

Schwarz, M.P., Barovich, K. and Hand, M., 2002. A plate margin setting for the evolution of the southern Gawler Craton: evidence from detrital zircon and Sm-Nd isotopic data of the Hutchison group. In: 16<sup>th</sup> Australian Geological Convention, Adelaide, 2002. Geological Society of Australia, Abstracts, 67, p70.

Schwarz, M.P., in. prep. Lincoln map sheet. Office of Minerals and Energy of South Australia. Geological Atlas 1:250 000 Series, sheet SH53-11.

Simpson, C.A., 1994. Constraints on Proterozoic crustal evolution from an isotopic and geochemical study of clastic sediments of the Gawler Craton, South Australia. University of Adelaide. B.Sc. (Hons) thesis (unpublished).

Taylor, S.R. & McLennan, S.M., 1985. *The Continental Crust: its composition and evolution. An examination of the geochemical record preserved in sedimentary rocks.* Blackwell, Oxford. 312.

Teale, G.S., Schwarz, M.P. & Fanning, C.M., 2000. Potential for Archaean VHMS-style mineralisation and other targets in southern Eyre Peninsula. *MESA Journal*, 18 July 2000.

*Ailsa Woodhouse, 2002.*

Thomson, B.P., (Compiler), 1980. Geologicak map of South Australia. South Australia. Geological Survey. Maps of South Australia Series, 1:1 000 000.

Timmerman, M.J & Daly, J.S. 1995. Sm-Nd evidence for late Archaean crust formation in the Lapland-Kola Mobile Belt, Kola Peninsul, Russia and Norway. *Precambrian Research*. 72, 97-107.

Toulkeridis, T., Clauer, N., Kroener, A., Reimer, T. Todt, W. 1999. Characterization, provenance, and tectonic setting of Fig Tree greywackes from the Archaean Barberton greenstone belt, South Africa. *Sedimentary Geology*. 124, 113-129.

Turner, S., Foden J., Sandiford, M., Bruce, D., 1993. Sm-Nd isotopic evidence for the provenance of sediments from the Adelaide fold belt and southeastern Australia with implications for episodic crustal addition. *Geochimica et Cosmochimica Acta*. 57; 8, 1837-1856.

Webb, A.W., Thomsom, B.P., Blissett, A.H., Daly, S.J., Flint, R.B and Parker, A.J., 1986. Geochronology of the Gawler Craton, South Australia. *Australian Journal of Earth Sciences*, 33, 119-143.

White, J.C., Urbanczyk, K.M., 2001. Origin of a silica-oversaturated quartz trachyret-rhyolite suite through combined crustal melting, magma mixing and fractional crystallization; the Leyva Canyon Volcano, Trans-Pecos magmatic province. Texas. *Journal of Volcanology and Geothermal Research*. 111, 155-182.

Whitehouse. M. J., Kamber, B.S. & Moorbath. S. 1999. Age significance of U-Th-Pb zircon data from early Archaean rocks of west Greenland-a reassessment based on combined ion-microprobe and imaging studies. *Chemical Geology*. 160, 201-224.

Williams, I.S., 1998. U-Th-Pb geochronology by ion microprobe. In: McKibben, M.A., Shanks III, W.C., Ridley, W.I. (Eds), *Applications of Microanalytical Techniques to understanding Mineralizing Processes*, *Reviews in Economic Geology*, 7, 1-35.

*Ailsa Woodhouse, 2002.*

Winter, J.D. 2001. An introduction to igneous and metamorphic petrology. Prentice Hall Inc. p 697

Wolf, M.B. and London, D. 1994. Apatite dissolution into peraluminous haplogranitic melts: An experimental; study of solubilities and mechanisms. *Geochim. Cosmochim. Acta.* 58 (19), 4127-4146.

Wolf, M.B. and London, D. 1995. Incongruent dissolution of REE- and Sr-rich apatite in peraluminous granitic liquids: Differential apatite, monazite and xenotime solubilities during anatexis. *Am. Mineral.* 80(7-8), 765-775.

Wyman, D.A. 1999. A 2.7 Ga depleted tholeiite suite: evidence of plume-arc interaction in the Abitibi Greenstone Belt, Canada. *Precambrian Research.* 97, 27-42.

### *Figure Captions*

Figure 1. The regional geology of South Australia showing the position of the Gawler Craton. Inset (a) shows the location of Figure 2, and the late Archaean to early Palaeoproterozoic Sleaford Complex in the southern Gawler Craton. Inset (b) shows the location of Mulgathing Complex in the central and northern Gawler Craton.

Figure 2. Interpreted subsurface geology of southern Eyre Peninsula (modified from Schwarz, in prep.) showing sampling localities for this study and previous studies. Wangary Gneiss; (a) Schaefer (1998), (b) & (c) this study, Fanning (1997) and Rich (2000). Hall Bay Volcanics; (d) Teale et al., 2000 and M.E.R. data in.prep. Carnot paragneisses; (e) this study, (f) Fanning, 1997 and Schaefer (1998).

Figure 3. (a) Combined histogram and relative probability distribution of detrital zircon age spectra from the Wangary Gneiss (sample A2030-2). (b) Combined histogram and relative probability distribution with measured Th/U ratios of detrital zircon analyses.

Figure 4. Cathodoluminescence (C.L.) images of representative detrital zircons from Wangary Gneiss sample A2030-2, showing locations and ages of the analyzed spots For each grain the

*Ailsa Woodhouse, 2002.*

analysis number is circled and number in the rectangle is the interpreted  $^{207}\text{Pb}/^{206}\text{Pb}$  age in Ma.

(a) Representative zircons with Th/U ratios  $< 0.2$ . (b) Representative zircon analyses *ca* 2480-2500 Ma. (c) Representative of zircon analyses *ca* 2510-2580 Ma; (d) representative of zircon analyses 2600-3120 Ma.

Figure 5. Combined histograms and relative probability distributions of U-Pb zircon analyses from the Hall Bay Volcanics, filtered to  $< 10\%$  discordance (M.E.R. data, in. prep.); (a) sample R432969; (b) sample R432967 (c) sample R43967 with measured Th/U ratios.

Figure 6. Harker diagram plots of the Wangary Gneiss, Carnot paragneiss and Hall Bay Volcanics.

Figure 7. Spider diagram of the Wangary Gneiss and Carnot paragneisses normalized to average Archaean mudstone (Taylor and McLennan, 1985).

Figure 8. Spider diagram of the Wangary Gneiss, Carnot paragneiss and Hall Bay Volcanics to normalized to primordial mantle (McDonough et al., 1992).

Figure 9. Harker-type Cr, Ni, V, Sc, Th, Ba and Sr variation diagrams for the Wangary Gneiss, Carnot paragneiss and Hall Bay Volcanics.

Figure 10. Chondrite-normalised REE diagrams of the Wangary Gneiss, Carnot paragneiss and Hall Bay Volcanics (Taylor and McLennan, 1985).

Figure 11. Initial  $\epsilon_{\text{Nd}}$  vs time diagram for the Wangary Gneiss, Carnot paragneiss and Hall Bay Volcanics. *DM* = depleted mantle evolution curve and *CHUR* = Chondrite normalized earth (Goldstein et al., 1985).

Figure 12. (a) Typical chondrite-normalized REE patterns for the basaltic and felsic endmembers of Archaean bimodal igneous rock suites and the average Archaean mudstone derived from 1:1 mixture of mafic and felsic endmembers (Taylor and McLennan, 1985); (b) Plot of  $(\text{La}/\text{Yb})_{\text{N}}$  vs Cr for the Wangary Gneiss, Carnot paragneisses and Hall Bay Volcanics; (c) Revised REE mixing model for Sleaford metasediments.

*Ailsa Woodhouse, 2002.*

Figure 13. Depositional setting of the protoliths of the Wangary Gneiss, Carnot paragneisses and Hall Bay Volcanics. These sequences are proposed to be deposited on a rifting shallow marine basin, derived predominately from Late Archaean bimodal terrains.

Figure 1.

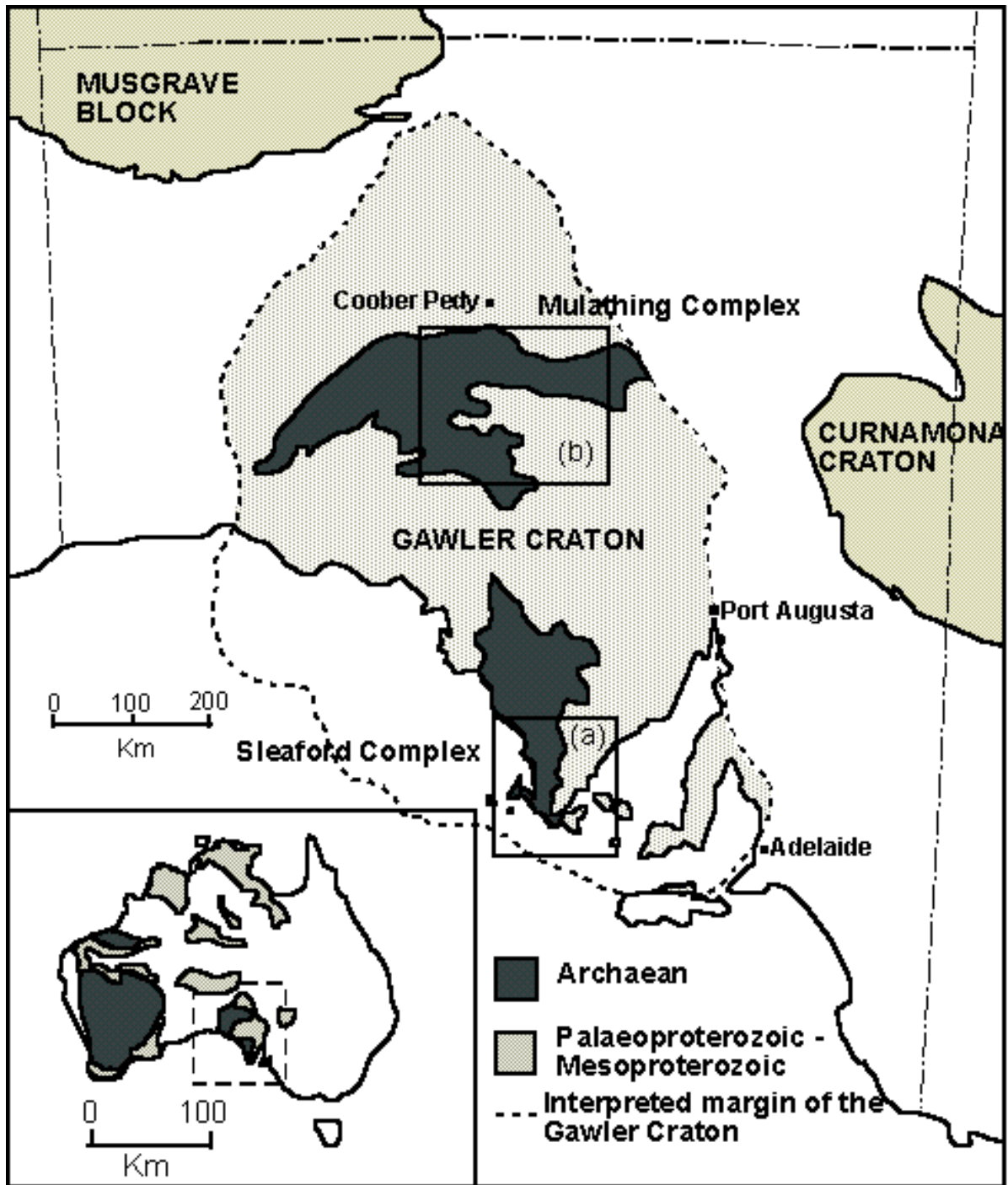


Figure 2.

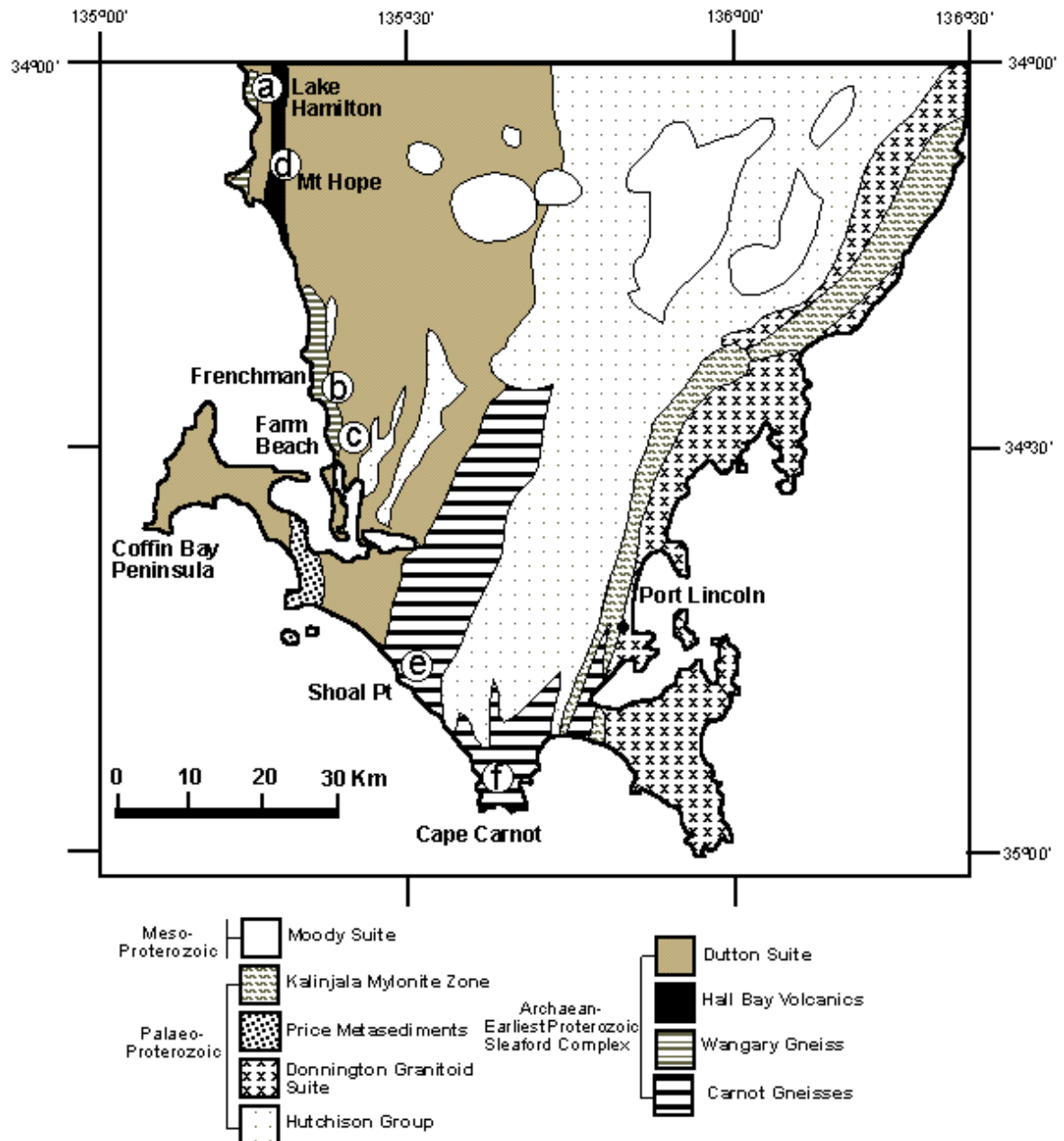
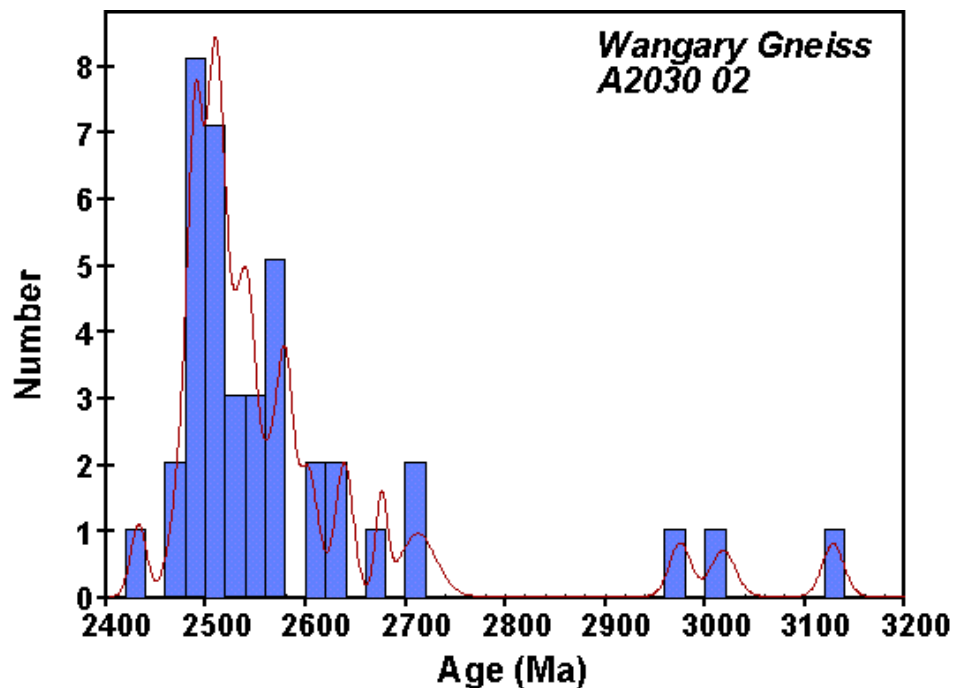


Figure 3.

(a)



(b)

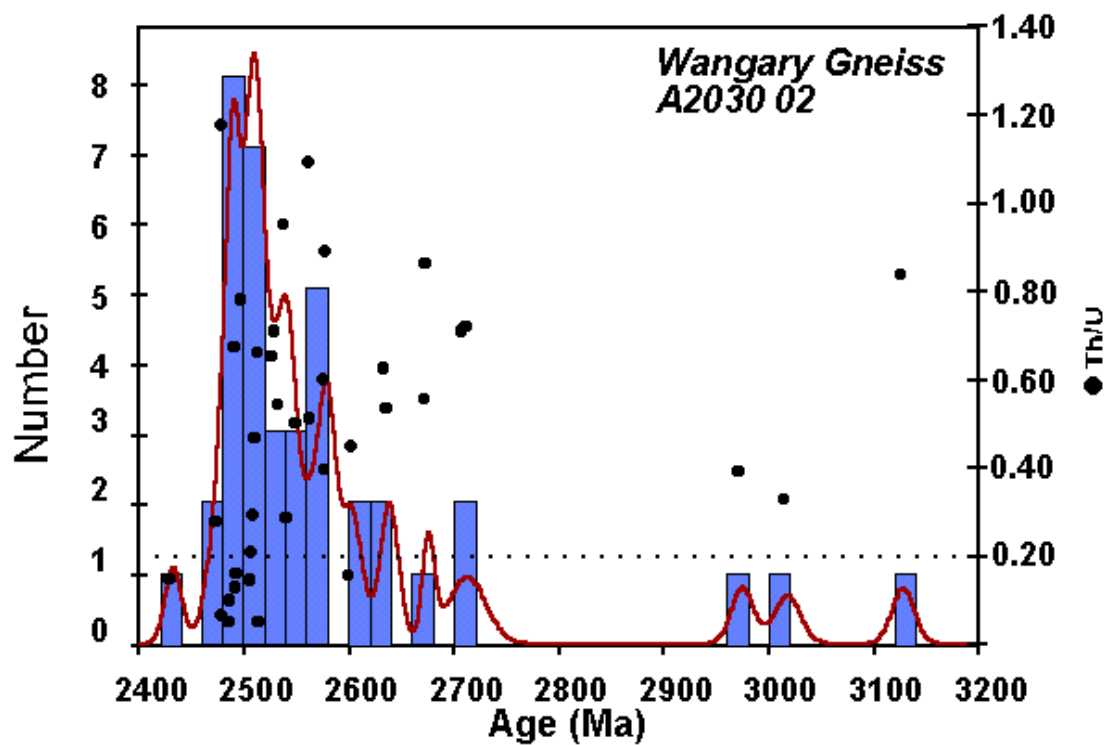
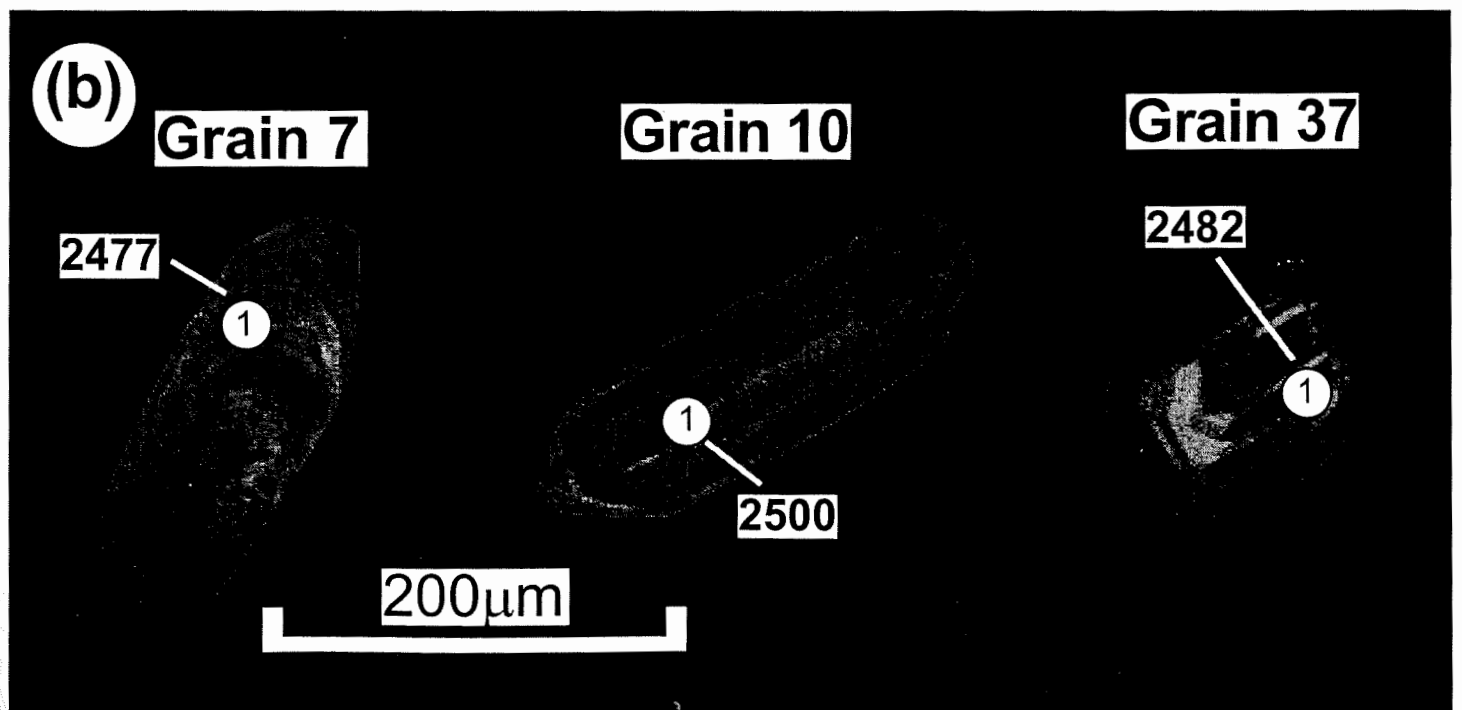
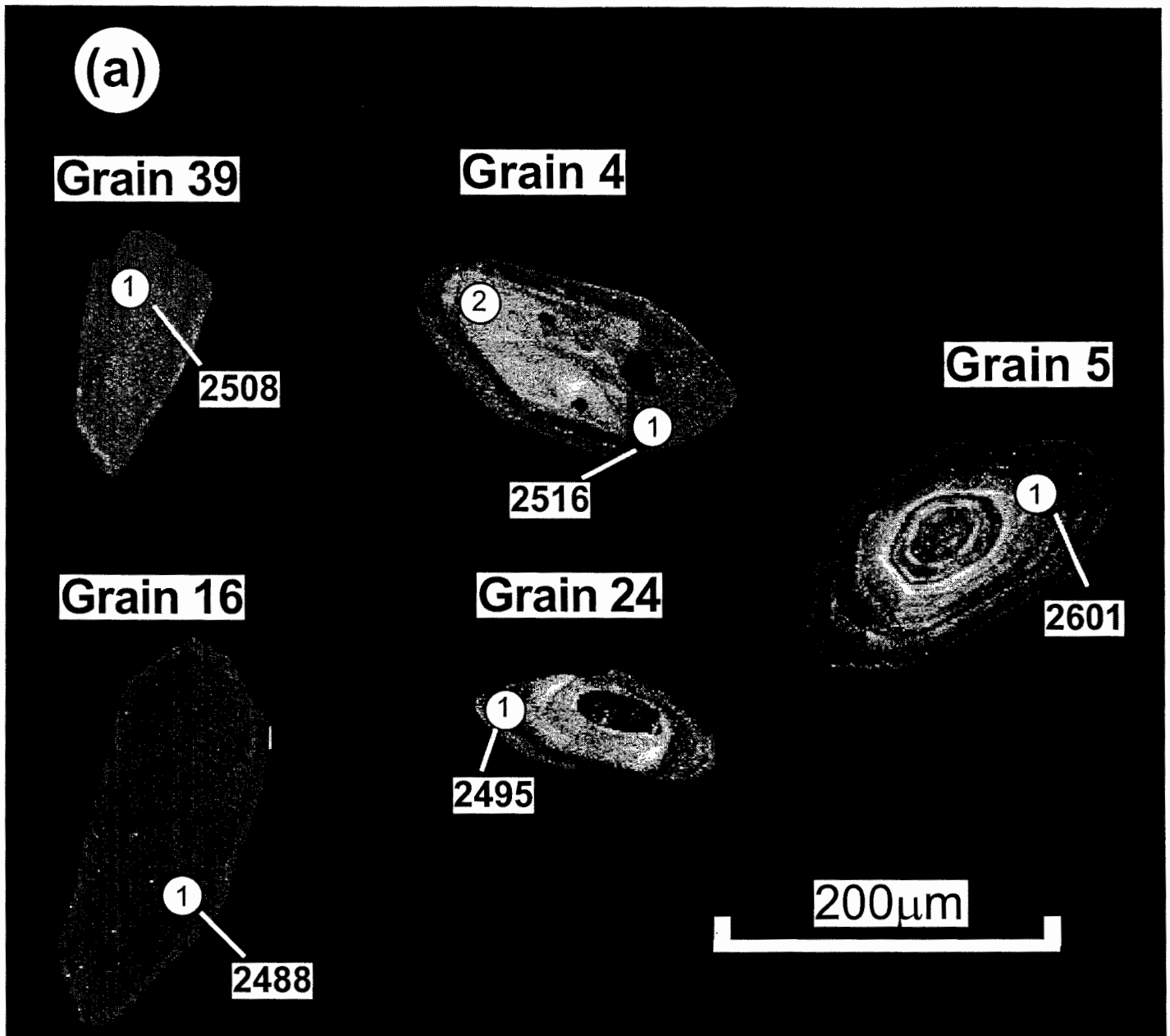


Figure 4



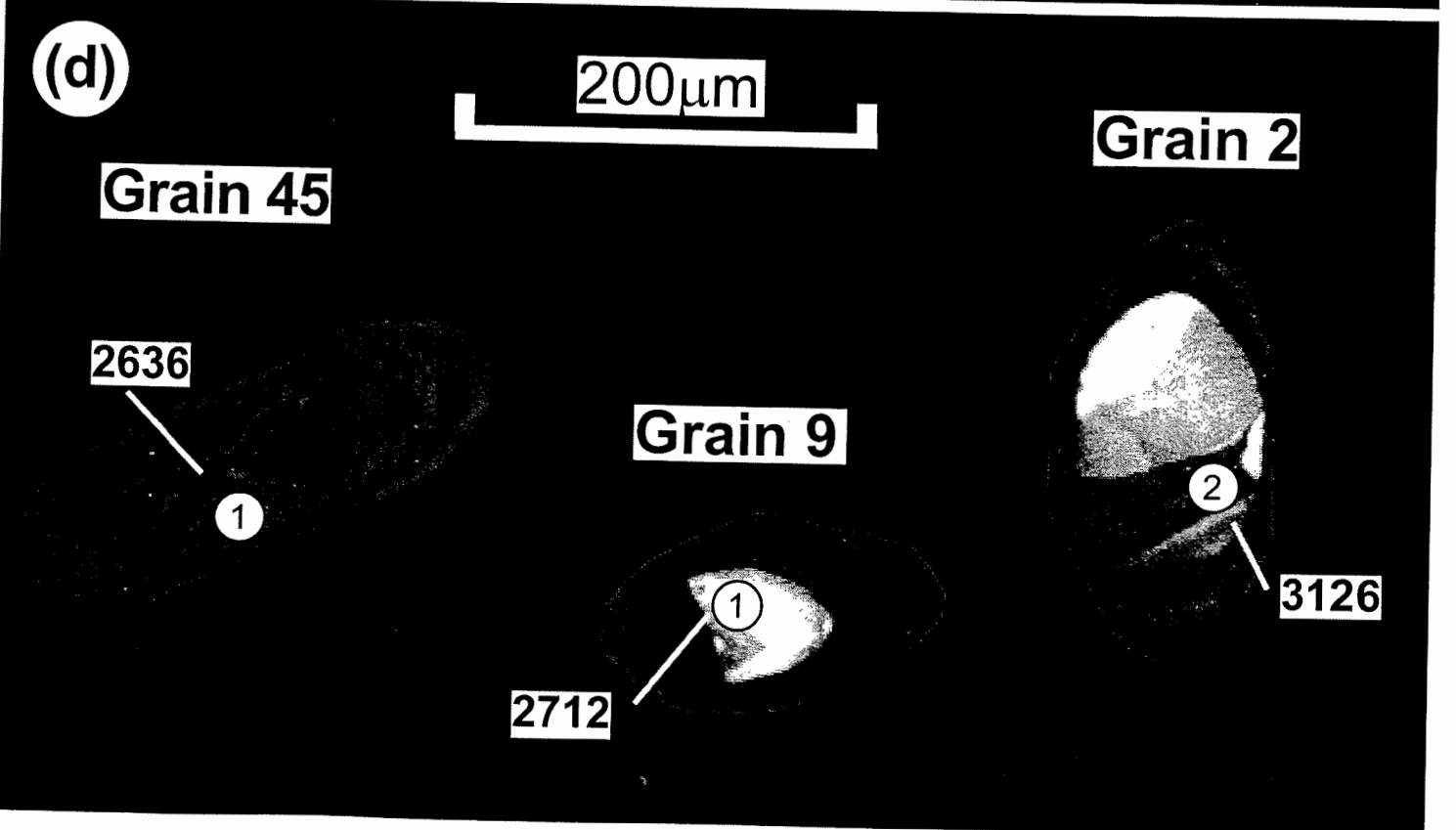
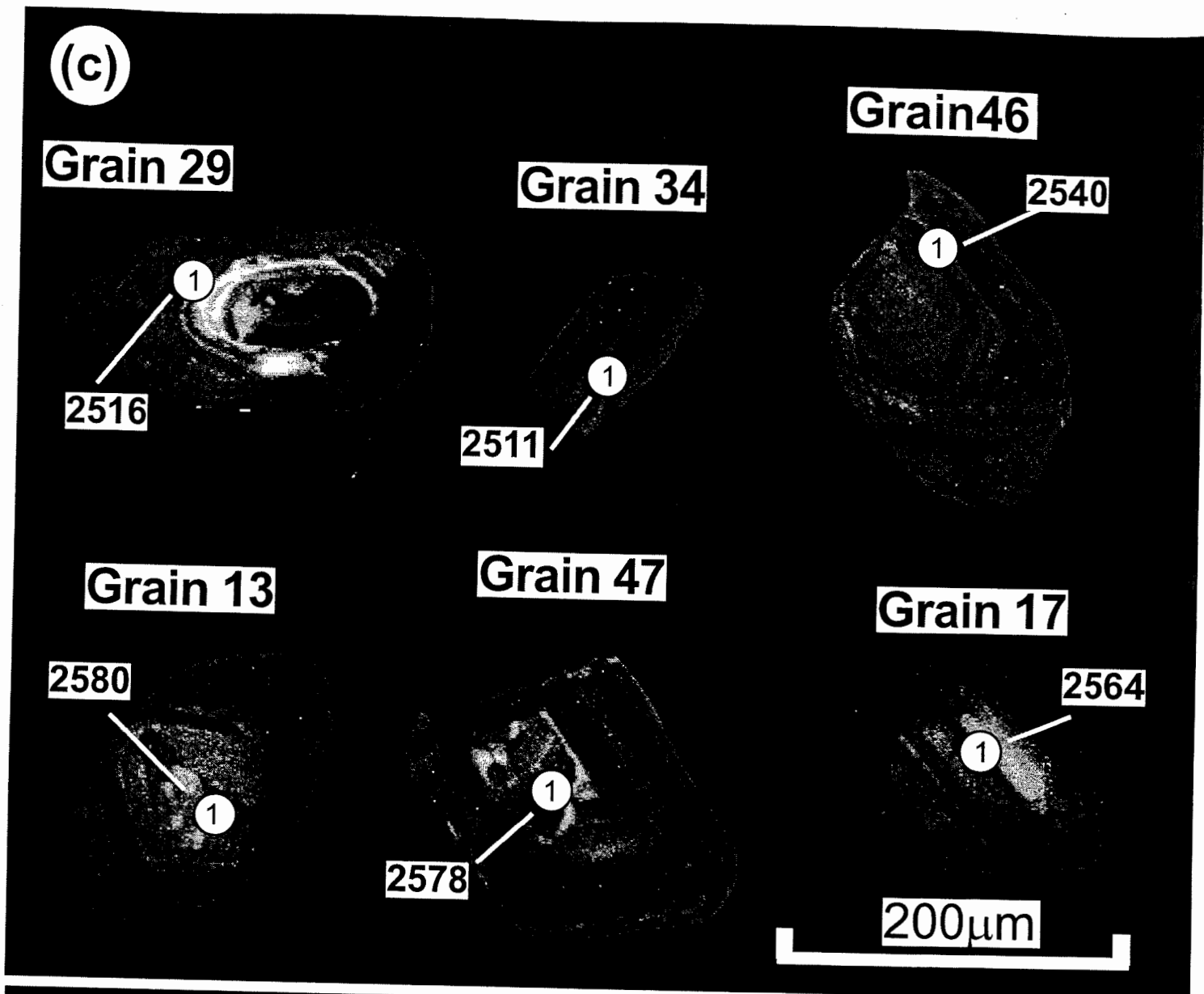
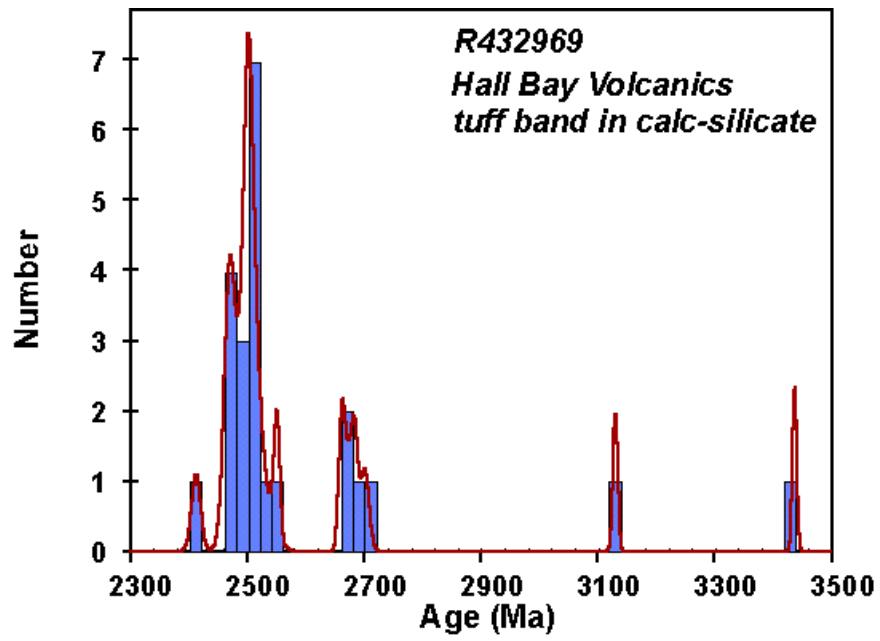


Figure 5.

(a)



(b)

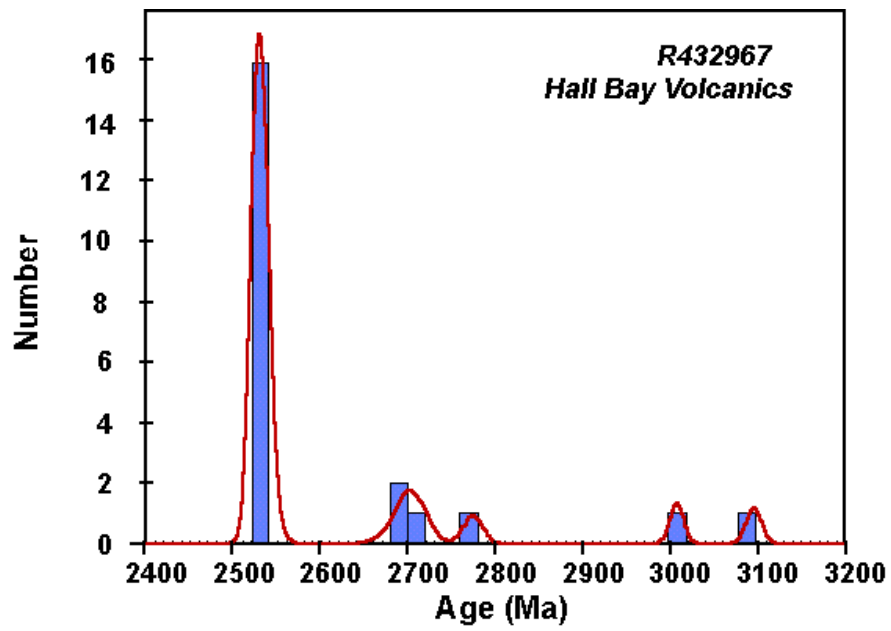


Figure 5(c)

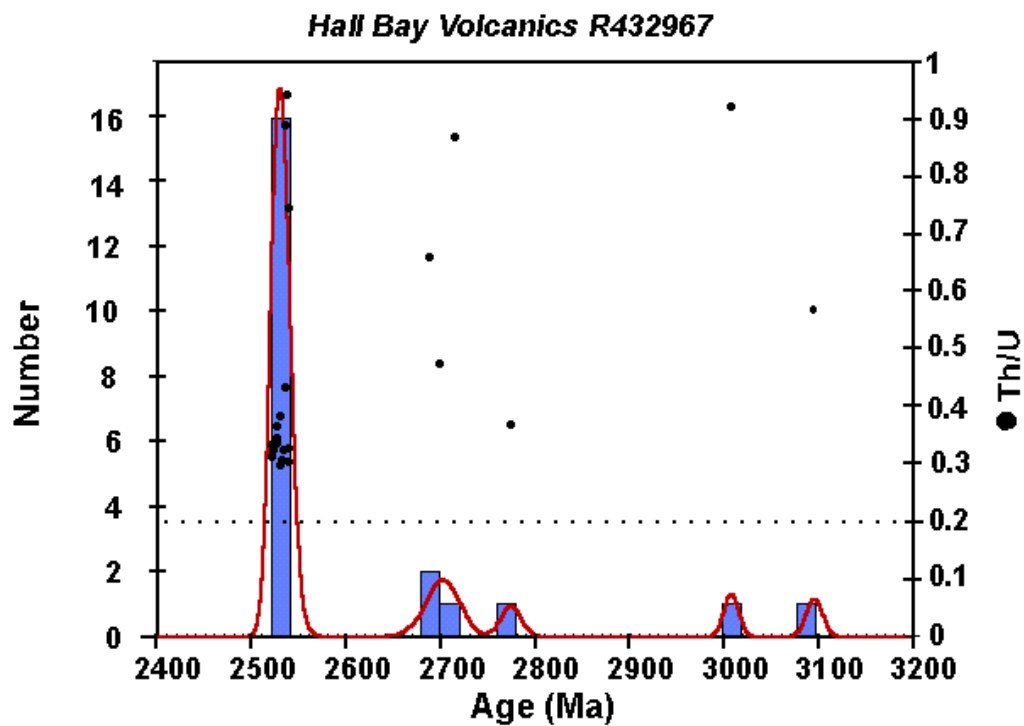


Figure 6.

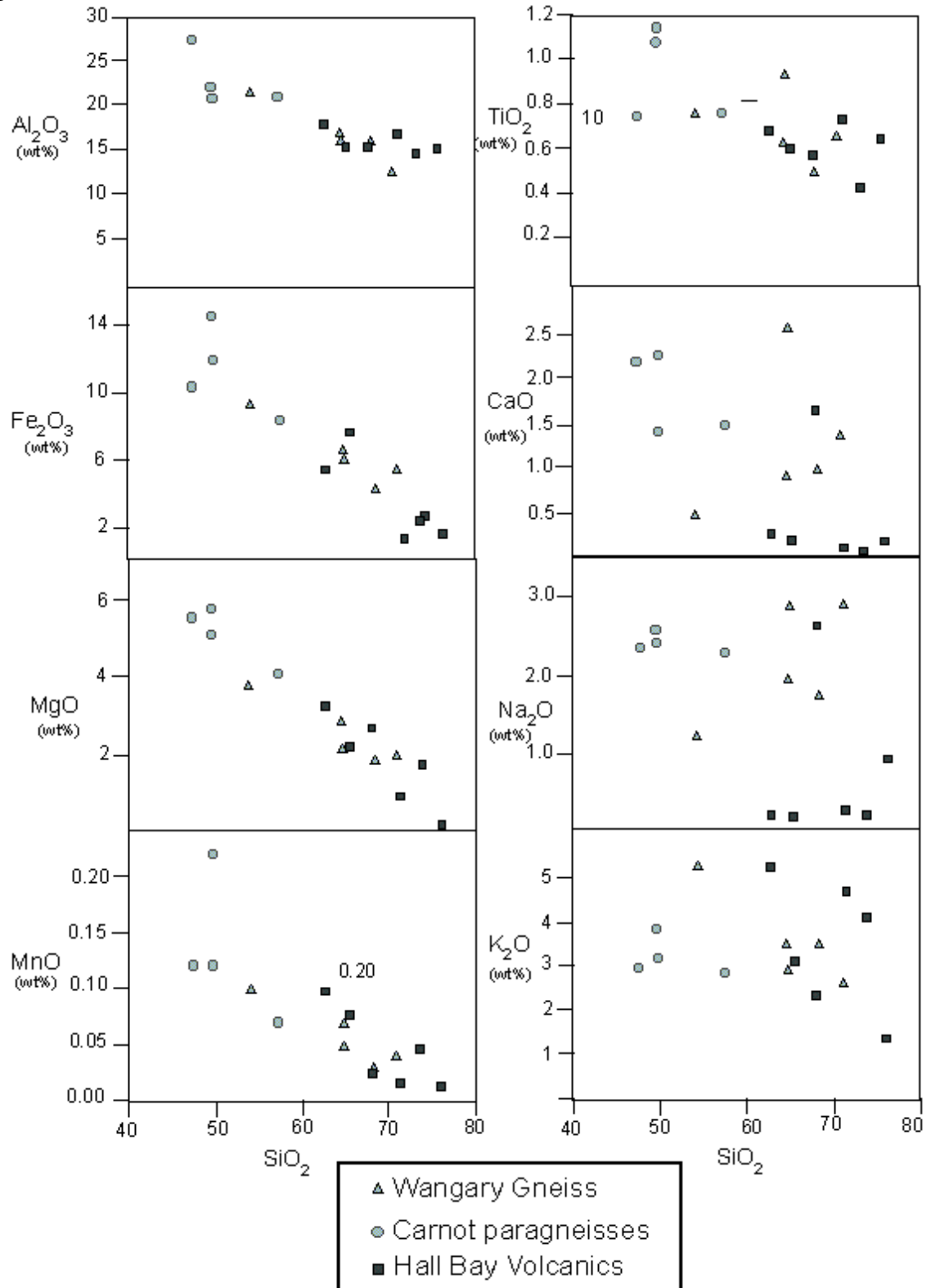


Figure 7.

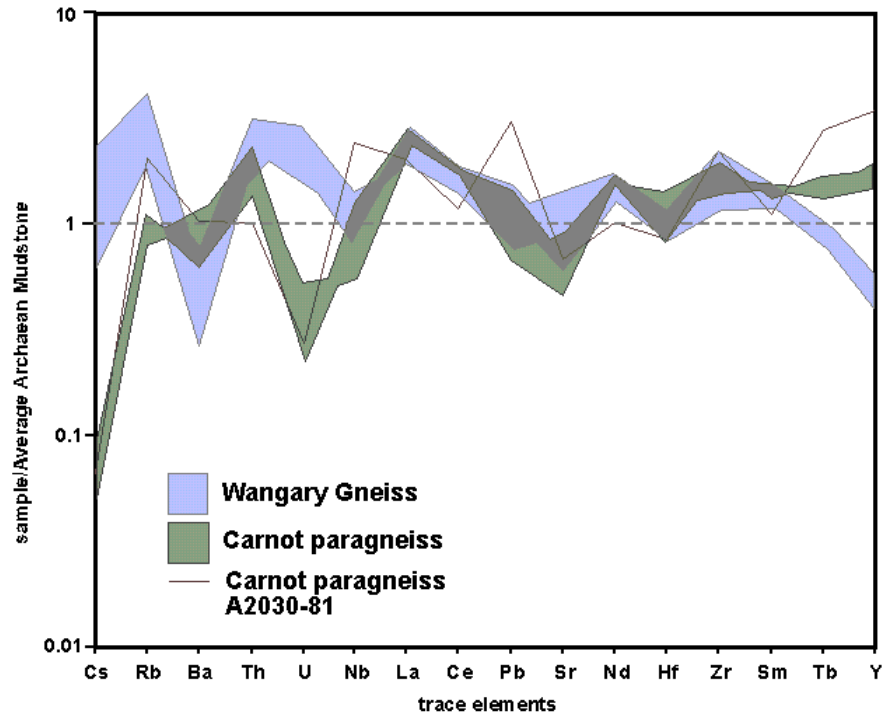


Figure 8.

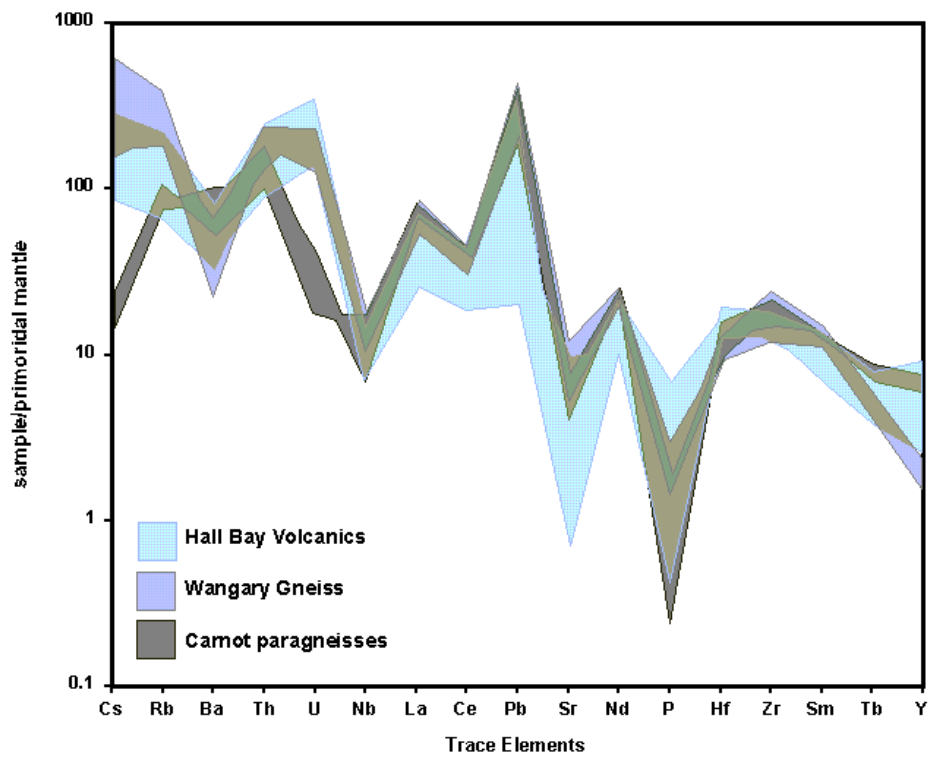


Figure 9.

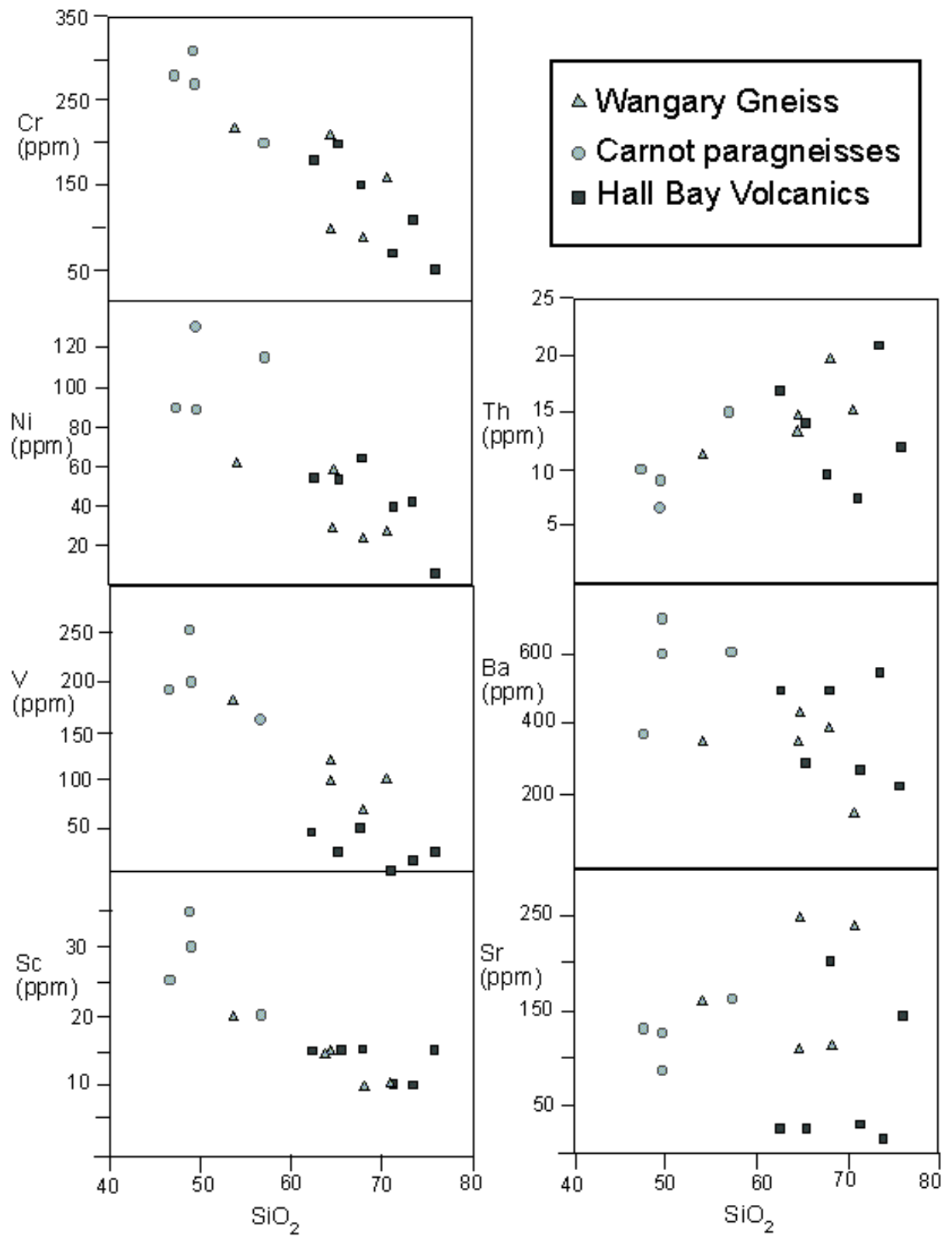


Figure 10.

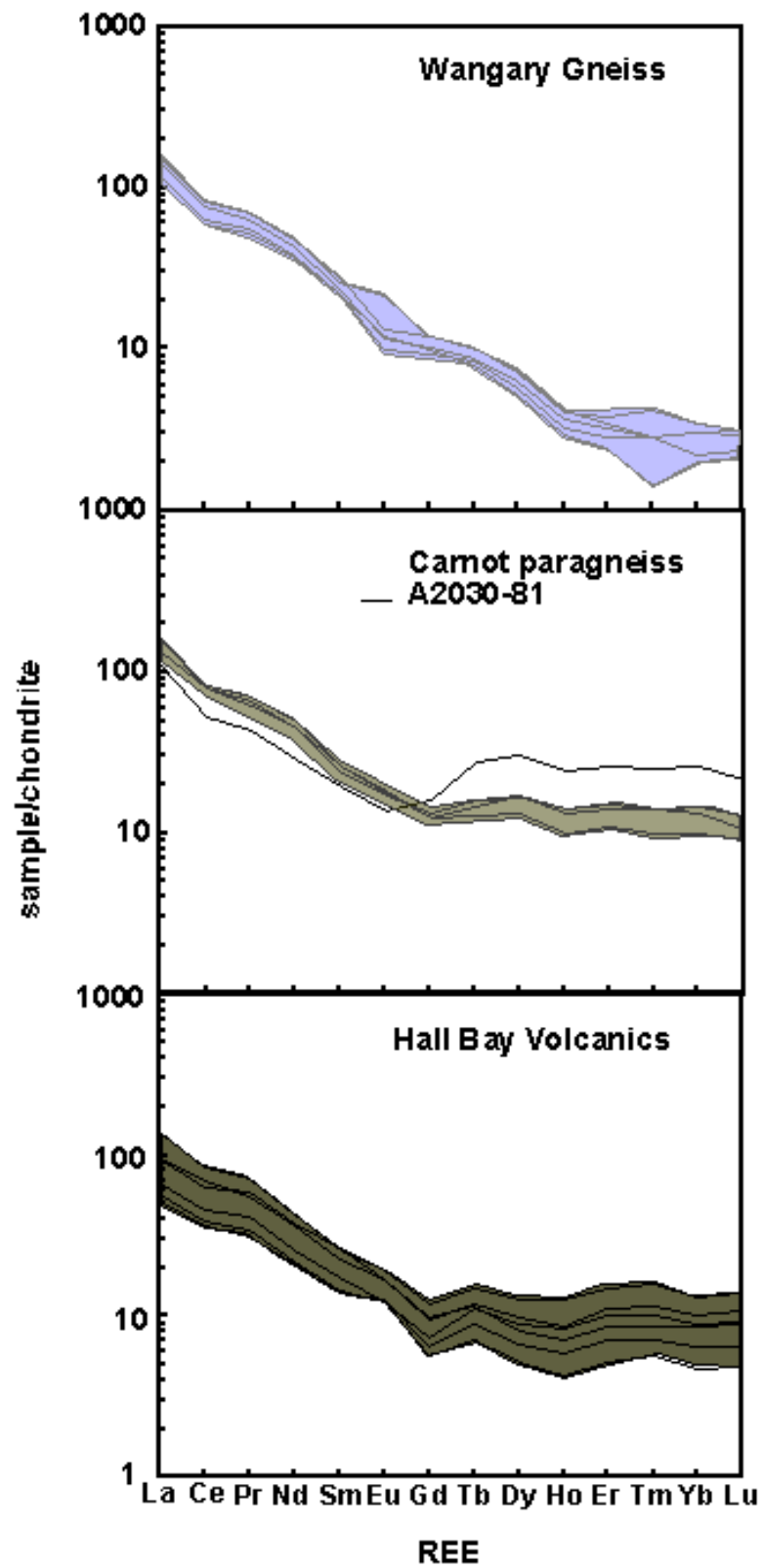


Figure 11.

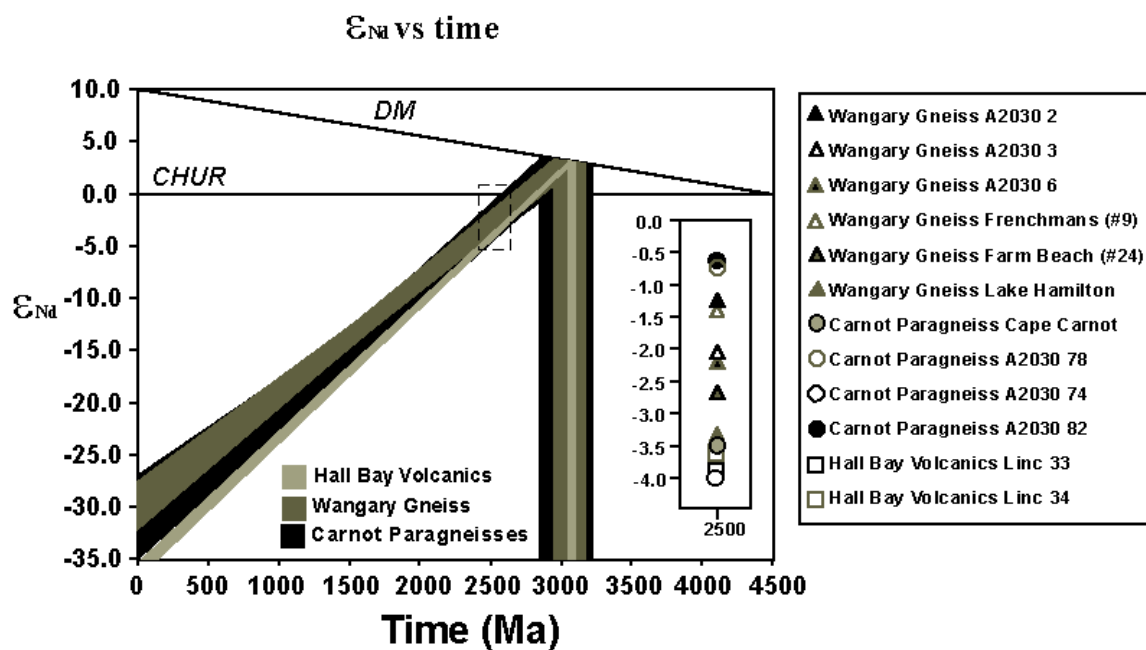
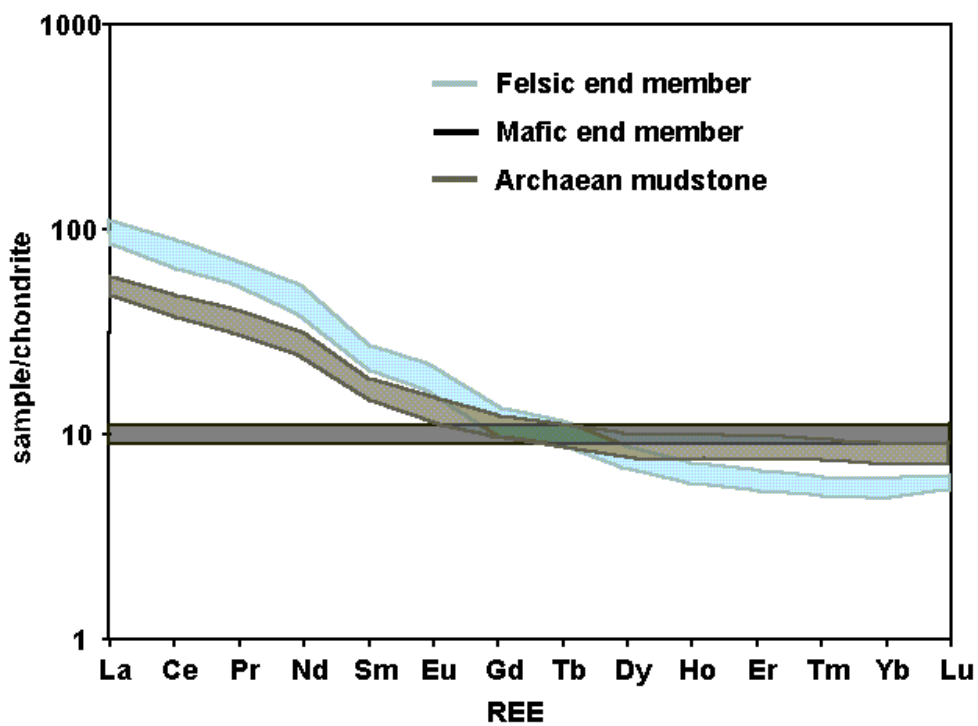
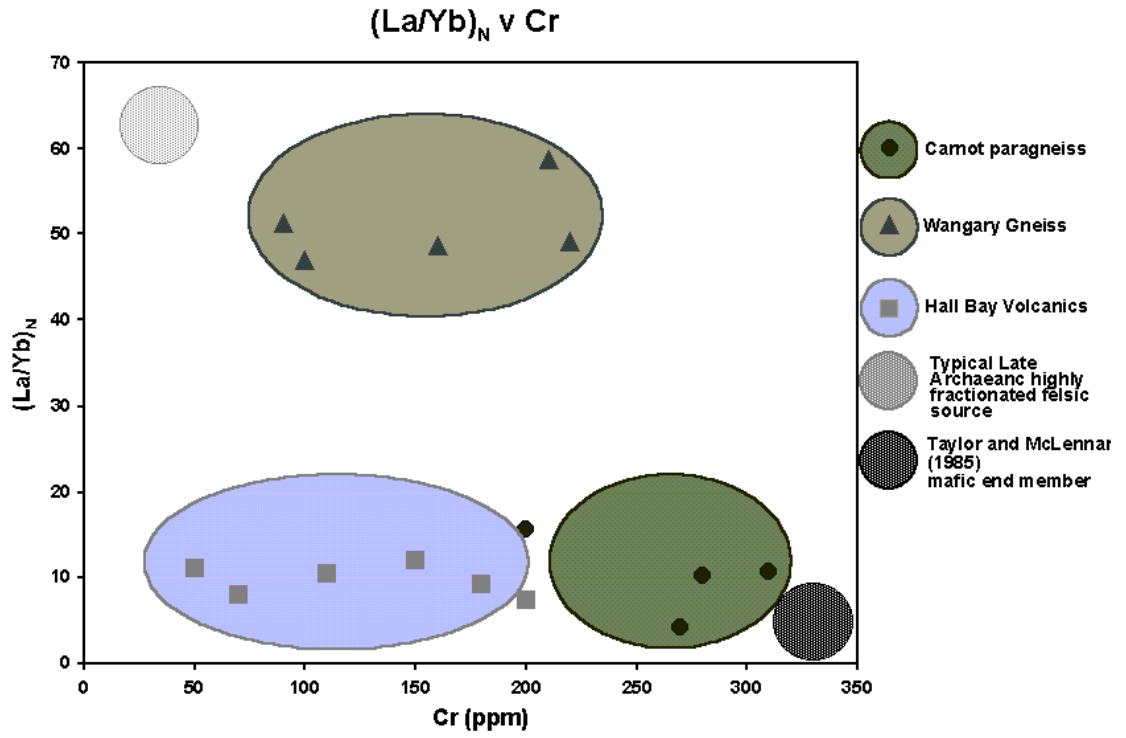


Figure 12(a)



Ailsa Woodhouse, 2002.  
Figure 12(b)



(c)

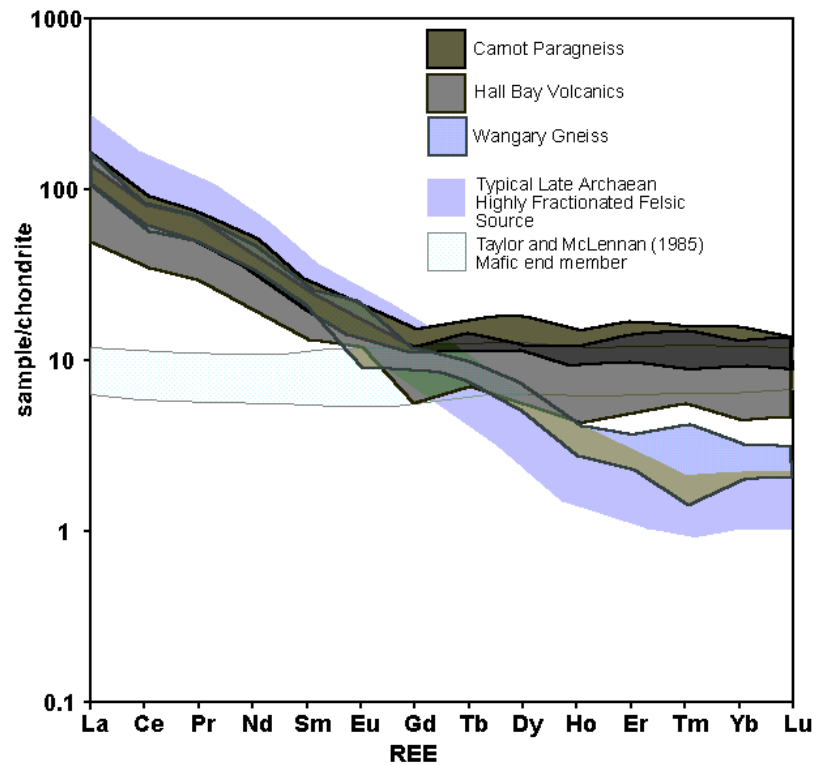


Figure 13.

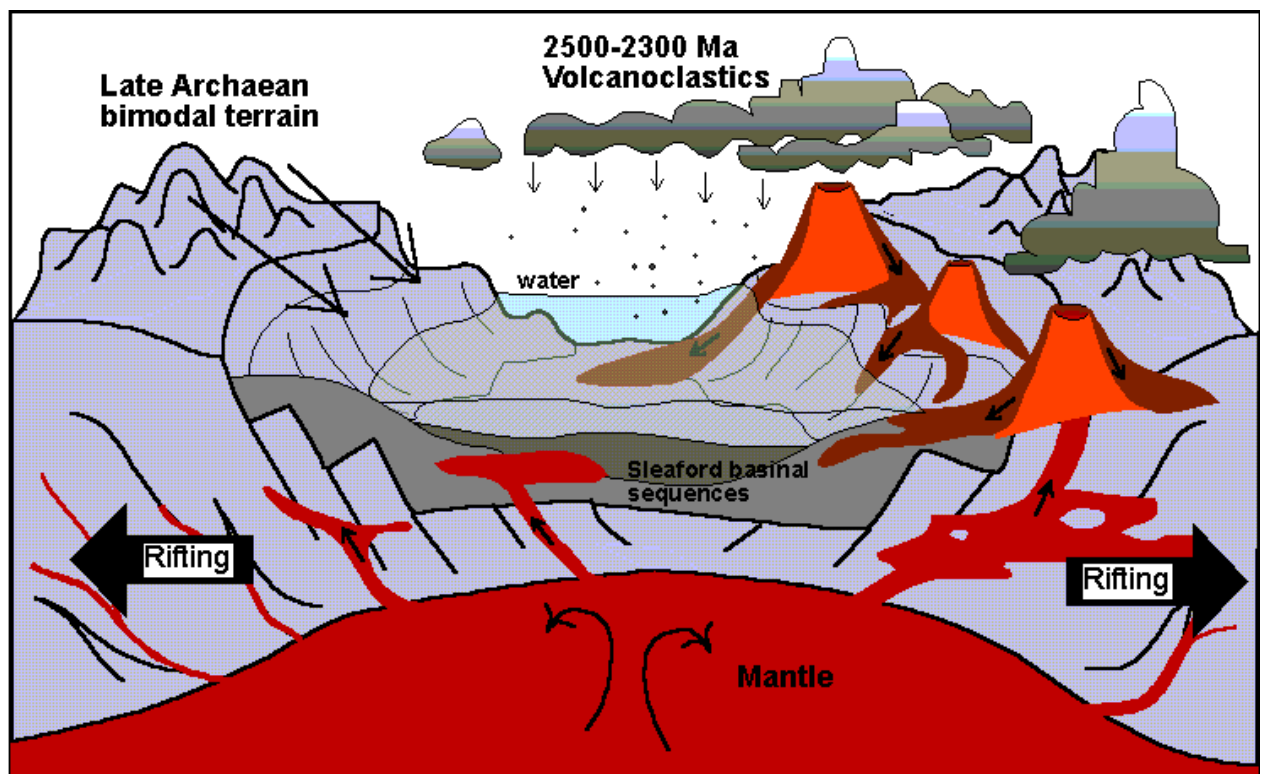


Table 1. Whole Rock Sm-Nd isotopes of the Gawler Archaean units (previous work)

Errors on  $^{143}\text{Nd}/^{144}\text{Nd}$  measurements are within  $2\sigma$  (mean) and refer to the last significant figures.  $\epsilon_{\text{Nd}}$  values calculated with CHUR (Goldstein et al, 1984) and depleted mantle model ages ( $T_{\text{DM}}$ ) from Goldstein et al, 1984 depleted mantle model curve.

Unit	Nd	Sm	$^{143}\text{Nd}/^{144}\text{Nd}$	$^{147}\text{Sm}/^{144}\text{Nd}$	Strat age (T)	$\epsilon_{\text{Nd}}(0)$	$\epsilon_{\text{Nd}}(T)$	$T_{\text{DM}}$	Reference
Hall Bay Volcanics									
Linc 33 Lake Hamilton	41.3	6.6	$0.51077\pm 7$	0.096	2520 Ma	-36.50	-3.9	3085 Ma	(M.E.R data inprep)
Linc 33 Lake Hamilton	24.0	3.8	$0.51082\pm 1$	0.098	2520 Ma	-35.50	-3.6	3072 Ma	(M.E.R data in prep)
Wangary Gneiss									
Lake Hamilton	53.1	9.9	$0.51106\pm 8$	0.112	2520 Ma	-30.74	-3.4	3140 Ma	(Schaefer, 1998)
(#9) Frenchmans	35.6	6.2	0.510960	0.100	2520 Ma	-32.75	-1.4	2938 Ma	(Rich, 2000)
(#24) Farm Beach	41.3	7.9	0.511228	0.120	2520 Ma	-27.50	-2.7	3131 Ma	(Rich, 2000)
Carnot paragneiss									
Cape Carnot	29.4	5.9	$0.51123\pm 5$	0.122	2520 Ma	-27.49	-3.5	3213 Ma	(Schaefer, 1998)

Table 2. Age constraints for Late Archaean evolution of the Gawler Craton. Relative abundances of zircon populations are not published.

Unit	SHRIMP U-Pb zircon population ages	Reference
Sleaford Complex		
Wangary Gneiss 5928 RS138 Farm Beach	<i>ca</i> 2480 Ma (interp metamorphic) $2679 \pm 9$ Ma (3 analyses)	Fanning (1997)
Carnot cordierite garnet paragneiss 516/464 Cape Carnot	2300 Ma to 2850 Ma (continuum of data) 2950 to 3150 Ma (a few analyses)	Fanning (1997)
Carnot hypersthene gneiss 516/414 Cape Carnot	<i>ca</i> 2400 Ma (interp metamorphic) <i>ca</i> 2500-2600 Ma (dominant)	Fanning (1997)
Kiana Granite Lake Hamilton	$2460\pm 15$ Ma $2557\pm 27$ Ma	Fanning (1997)
Coulta Granodiorite	$2517\pm 14$ Ma	Fanning (1997)
Hall Bay Volcanics Lake Hamilton	<i>ca</i> 2520 Ma magmatic age 2720 Ma inheritance	Teale et al., (2000)
Unit	Rb-Sr Isochron	Reference
Augen Gneiss Cape Carnot	$2436\pm 137$ Ma	Daly and Fanning (1993)
Whidbey Granite	$2337\pm 71$ Ma	Webb et al (1986)

Table 3. SHRIMP U-Pb zircon results for Hall Bay Volcanics sample R 432 697, samples with discordance > 10% were excluded from histograms and relative probability distributions.

Table xyz. Summary of SHRIMP U-Pb zircon results for samples R432967, Hall Bay Volcanics (LINC30).																		
Grain spot	U (ppm)	Th (ppm)	Th/U	<sup>206</sup> Pb* (ppm)	<sup>204</sup> Pb/ <sup>206</sup> Pb	f206 %	Radiogenic Ratios						Age (Ma)					
							<sup>206</sup> Pb/ <sup>238</sup> U ±	<sup>207</sup> Pb/ <sup>235</sup> U ±	<sup>207</sup> Pb/ <sup>206</sup> Pb ±	r	<sup>206</sup> Pb/ <sup>238</sup> U ±	<sup>207</sup> Pb/ <sup>206</sup> Pb ±	% Disc					
1.1	88	42	0.47	39	0.000063	0.09	0.5179	0.0063	13.209	0.188	0.1850	0.0013	0.863	2690	27	2698	12	0
2.1	95	35	0.37	43	0.000100	0.14	0.5212	0.0064	13.922	0.196	0.1937	0.0013	0.870	2704	27	2774	11	3
3.1	253	86	0.34	102	0.000068	0.10	0.4695	0.0042	10.768	0.111	0.1664	0.0009	0.868	2481	18	2521	9	2
4.1	139	131	0.94	56	0.000217	0.30	0.4649	0.0056	10.766	0.157	0.1680	0.0014	0.833	2461	25	2537	14	3
5.1	276	94	0.34	113	0.000053	0.07	0.4763	0.0038	10.957	0.100	0.1668	0.0007	0.886	2511	17	2526	7	1
6.1	244	94	0.38	100	0.000038	0.05	0.4782	0.0058	11.019	0.142	0.1671	0.0007	0.944	2520	25	2529	7	0
7.1	228	169	0.74	103	0.000098	0.12	0.5265	0.0045	18.956	0.185	0.2611	0.0012	0.874	2727	19	3254	7	19
8.1	192	143	0.75	72	0.000116	0.16	0.4338	0.0039	10.053	0.107	0.1681	0.0010	0.845	2323	18	2539	10	9
9.1	264	78	0.30	104	0.000087	0.12	0.4585	0.0038	10.564	0.100	0.1671	0.0008	0.877	2433	17	2529	8	4
10.1	300	141	0.47	107	0.000169	0.24	0.4160	0.0042	9.604	0.108	0.1675	0.0008	0.900	2242	19	2532	8	13
11.1	244	79	0.32	98	0.000085	0.12	0.4659	0.0039	10.766	0.104	0.1676	0.0008	0.878	2466	17	2534	8	3
12.1	271	99	0.37	101	0.000065	0.09	0.4343	0.0035	9.997	0.092	0.1670	0.0007	0.877	2325	16	2527	7	9
13.1	128	118	0.92	65	0.000125	0.16	0.5870	0.0062	18.104	0.210	0.2237	0.0011	0.903	2977	25	3007	8	1
14.1	98	85	0.87	43	0.000230	0.31	0.5109	0.0059	13.172	0.183	0.1870	0.0015	0.826	2660	25	2716	13	2
15.1	184	163	0.89	71	0.000113	0.16	0.4523	0.0042	10.455	0.112	0.1676	0.0009	0.860	2406	19	2534	9	5
16.1	243	79	0.33	100	0.000036	0.05	0.4771	0.0041	10.950	0.102	0.1665	0.0006	0.913	2515	18	2522	6	0
12.2	306	105	0.34	127	0.000040	0.06	0.4814	0.0040	11.073	0.101	0.1668	0.0006	0.910	2533	17	2526	6	0
17.1	198	61	0.31	81	0.000005	0.01	0.4779	0.0063	11.023	0.152	0.1673	0.0007	0.952	2518	27	2531	7	1
18.1	249	108	0.43	97	0.000075	0.10	0.4542	0.0038	10.504	0.099	0.1677	0.0007	0.889	2414	17	2535	7	5
19.1	190	58	0.31	78	0.000021	0.03	0.4770	0.0042	11.056	0.109	0.1681	0.0007	0.904	2514	19	2539	7	1
20.1	36	24	0.66	17	0.000195	0.27	0.5520	0.0075	14.001	0.246	0.1839	0.0020	0.777	2834	31	2689	18	-5
21.1	285	91	0.32	116	0.000035	0.05	0.4758	0.0039	10.907	0.098	0.1662	0.0006	0.920	2509	17	2520	6	0
22.1	257	85	0.33	101	-	<0.01	0.4582	0.0038	10.607	0.098	0.1679	0.0007	0.906	2431	17	2537	7	4
23.1	498	563	1.13	87.7	0.001635	2.28	0.2004	0.0021	4.710	0.100	0.1704	0.0032	0.485	1178	11	2562	31	118
17.2	492	558	1.13	100.0	0.001313	1.72	0.2324	0.0024	6.792	0.111	0.2119	0.0027	0.630	1347	13	2920	21	117
24.1	837	994	1.19	140.4	0.003221	4.62	0.1863	0.0041	3.961	0.205	0.1542	0.0072	0.429	1101	22	2393	80	117
25.1	379	269	0.71	108.7	0.000792	1.11	0.3299	0.0034	7.623	0.109	0.1676	0.0017	0.720	1838	17	2534	17	38
26.1	393	177	0.45	119.0	0.000228	0.32	0.3514	0.0037	7.920	0.092	0.1635	0.0009	0.894	1941	17	2492	9	28
27.1	370	216	0.58	102.9	0.000840	1.18	0.3201	0.0041	7.333	0.123	0.1661	0.0018	0.770	1790	20	2519	18	41
28.1	95	54	0.57	49.8	0.000150	0.19	0.6109	0.0081	19.907	0.286	0.2363	0.0013	0.919	3074	32	3095	9	1

Notes :

1. Uncertainties given at the one s level.
2. f206 %denotes the percentage of <sup>206</sup>Pb that is common Pb.
3. Correction for common Pb made using the measured <sup>204</sup>Pb/<sup>206</sup>Pb ratio.
4. For %Disc., 0%denotes a concordant analysis.

Table 4. Chemical composition of Hall Bay Volcanics. (M.E.R. data, in. prep.). (La/Yb)<sub>N</sub> and (Gd/Yb)<sub>N</sub> are chondrite normalized ratios; chondrite REE abundances from Taylor and McLennan (1985);  $Eu/Eu^* = 2 * Eu_N / (Sm_N + Gd_N)$ .

Lithology	Hall Bay Volcanics						
	Sample #	R433005	R433006	R433017	R433023	R433029	R433044
Eastings	527124	527007	526703	526600	526496	526111	
Northings	6227386	6227397	6227404	6227384	6227397	6221869	
Location	Line 29	Line 30	Line 31	Line 32	Line 33	Line 36	
SiO <sub>2</sub>	76	71.4	65.4	62.7	73.6	68	
TiO <sub>2</sub>	0.64	0.725	0.6	0.68	0.42	0.565	
Al <sub>2</sub> O <sub>3</sub>	15.3	16.8	15.5	18	14.6	15.5	
Fe <sub>2</sub> O <sub>3</sub>	1.59	1.33	7.62	5.29	2.37	4.13	
MnO	0.01	0.02	0.08	0.10	0.05	0.03	
MgO	0.21	0.91	2.2	3.27	1.73	2.7	
CaO	0.17	0.09	0.17	0.25	0.05	1.62	
Na <sub>2</sub> O	0.92	0.27	0.2	0.21	0.21	2.63	
K <sub>2</sub> O	1.38	4.71	3.1	5.23	4.11	2.29	
P <sub>2</sub> O <sub>5</sub>		0.02	0.07	0.14	0.03	0.12	
S							
LOI	2.49	2.95	3.4	3.56	2.88	1.88	
La	34.5	18.5	24	34.5	50	20.5	
Ce	60	34.5	43.5	66	78	36.5	
Pr	8	4.2	5.5	7.5	9.5	4.6	
Nd	26.5	14.5	18	25.5	30	15	
Sm	6	3.2	3.9	5	6	3.3	
Eu	1.45	1.1	1.05	1.45	1.65	1.05	
Gd	3	1.95	2.2	2.9	3.6	1.7	
Tb	0.66	0.51	0.64	0.69	0.85	0.41	
Dy	3	2.5	3.3	3.7	4.7	1.95	
Ho	0.6	0.49	0.71	0.72	1.05	0.36	
Er	2.1	1.75	2.5	2.7	3.7	1.25	
Tm	0.3	0.25	0.35	0.4	0.55	0.2	
Yb	2.1	1.55	2.2	2.5	3.2	1.15	
Lu	0.33	0.24	0.34	0.4	0.53	0.18	
(La/Yb) <sub>N</sub>	11.10	8.07	7.37	9.33	10.56	12.05	
Eu/Eu*	0.93	1.25	1.00	1.07	1.01	1.22	
(La/Sm) <sub>N</sub>	3.62	3.64	3.87	4.34	5.25	3.91	
(Gd/Yb) <sub>N</sub>	1.16	1.02	0.81	0.94	0.91	1.20	
Y	18	15	23	22	41.5	11.5	
Cr	50	70	200	180	110	150	
V	24	4	25	44	15	49	
Sc	15	10	15	15	10	15	
Ni	6	40	53	55	42	65	
Co	2	29	22	21	32	21	
Cu	3	13	35	21	6	38	
Zn	39	53	1400	290	135	34	
Cr/V	2.08	17.50	8.00	4.09	7.33	3.06	
V/Ni	4.00	0.10	0.47	0.80	0.36	0.75	
Ni/Co	3.00	1.38	2.41	2.62	1.31	3.10	
Cs	2	3	2.4	6.5	2.7	4.2	
Rb	41.5	100	93	140	84	79	
Tl	0.4	0.8	2.1	1.6	1.1	0.6	
Ba	230	270	290	500	550	500	
Pb	<3	<3	6	24	12	4	
Sr	145	30	25	25	15	200	
Th	12	7.5	14	17	21	9.5	
U	2.9	3.1	3.6	3.7	7	3	
Zr	200	150	140	140	150	160	
Hf	6	4	5	5	5	4	
Nb	<10	<10	10	10	<10	<10	
Mo	0.4	2.4	2.6	3.7	4.3	3.3	
W	<3	4	4	4	6	4	
Bi	0.3	0.2	0.2	1.9	1.9	0.2	
Zr/Hf	33.33	37.50	28.00	28.00	30.00	40.00	
Th/U	4.14	2.42	3.89	4.59	3.00	3.17	
La/Th	2.88	2.47	1.71	2.03	2.38	2.16	
Au	1	1	2	<1	<1	<1	
Ag	<0.5	<0.5	<0.5	<0.5	<0.5	<0.5	
As	1	34	7	19	25	32	
Be	4.5	1	4	1	2	1	
Ga	23	25.5	23.5	28.5	21	25.5	
Pr	8	4.2	5.5	7.5	9.5	4.6	

Table 5. SHRIMP U-Pb zircon results for Wangary Gneiss sample A2030-2, with discordance > 10% were excluded from histograms and relative probability distributions.

Table xyz. Summary of SHRIMP U-Pb zircon results for samples R445519, andalusite schist, The Frenchman.																		
Grain.	U	Th	Th/U	<sup>206</sup> Pb*	<sup>204</sup> Pb/	f206	Radiogenic Ratios						Age (Ma)					
							<sup>206</sup> Pb/	<sup>207</sup> Pb/	<sup>207</sup> Pb/	<sup>207</sup> Pb/	<sup>206</sup> Pb/	<sup>207</sup> Pb/	<sup>206</sup> Pb/	<sup>207</sup> Pb/	%			
spot	(ppm)	(ppm)		(ppm)	<sup>206</sup> Pb	%	<sup>238</sup> U	±	<sup>235</sup> U		<sup>206</sup> Pb	±	r	<sup>238</sup> U	±	<sup>206</sup> Pb	±	Disc
1.2	675	113	0.17	199	0.000103	0.14	0.3431	0.0041	7.747	0.109	0.3431	0.0041	0.854	1902	20	2495	12	31
2.2	382	321	0.84	194	0.000008	0.01	0.5899	0.0076	19.599	0.287	0.5899	0.0076	0.884	2989	31	3126	11	5
4.1	550	29	0.05	221	0.000074	0.10	0.4666	0.0057	10.673	0.141	0.4666	0.0057	0.926	2469	25	2516	8	2
4.2	199	90	0.45	86	0.000005	0.01	0.5007	0.0068	12.067	0.189	0.5007	0.0068	0.874	2617	29	2604	13	0
5.1	506	79	0.16	182	0.000082	0.11	0.4174	0.0051	10.042	0.132	0.4174	0.0051	0.926	2249	23	2601	8	16
6.1	779	77	0.10	240	0.000102	0.14	0.3587	0.0042	8.051	0.102	0.3587	0.0042	0.931	1976	20	2485	8	26
7.1	298	84	0.28	106	0.000114	0.16	0.4115	0.0054	9.194	0.136	0.4115	0.0054	0.878	2222	24	2477	12	11
7.2	540	525	0.97	169	0.000127	0.18	0.3646	0.0046	8.043	0.115	0.3646	0.0046	0.878	2004	22	2456	12	23
8.1	300	164	0.55	120	-	<0.01	0.4647	0.0060	10.743	0.153	0.4647	0.0060	0.910	2460	27	2534	10	3
9.1	78	57	0.72	34	-	<0.01	0.5123	0.0088	13.181	0.270	0.5123	0.0088	0.840	2666	38	2712	18	2
10.1	363	285	0.79	141	0.000021	0.03	0.4513	0.0062	10.219	0.152	0.4513	0.0062	0.923	2401	28	2500	10	4
11.1	362	245	0.68	142	0.000050	0.07	0.4573	0.0062	10.319	0.153	0.4573	0.0062	0.916	2428	27	2494	10	3
12.1	335	158	0.47	134	0.000065	0.09	0.4641	0.0060	10.593	0.149	0.4641	0.0060	0.911	2457	26	2513	10	2
13.1	212	190	0.89	89	0.000018	0.03	0.4854	0.0068	11.528	0.184	0.4854	0.0068	0.882	2551	30	2580	13	1
14.1	671	101	0.15	189	0.000190	0.27	0.3281	0.0042	7.405	0.114	0.3281	0.0042	0.832	1829	20	2494	14	36
15.1	162	54	0.33	82	0.000054	0.07	0.5851	0.0093	18.144	0.323	0.5851	0.0093	0.898	2970	38	3016	13	2
16.1	636	33	0.05	230	0.000037	0.05	0.4210	0.0054	9.466	0.132	0.4210	0.0054	0.922	2265	25	2488	9	10
17.1	138	151	1.09	53	0.000077	0.11	0.4488	0.0081	10.557	0.223	0.4488	0.0081	0.857	2390	36	2564	18	7
18.1	157	112	0.71	71	-	<0.01	0.5244	0.0095	13.463	0.285	0.5244	0.0095	0.857	2718	40	2709	18	0
19.1	343	60	0.17	109	0.000020	0.03	0.3695	0.0067	8.245	0.160	0.3695	0.0067	0.932	2027	32	2475	12	22
20.1	539	36	0.07	204	0.000073	0.10	0.4408	0.0049	9.876	0.116	0.4408	0.0049	0.947	2354	22	2482	6	5
21.1	796	82	0.10	145	0.001761	2.47	0.2072	0.0023	4.765	0.108	0.1668	0.0033	0.490	1214	12	2526	33	108
22.1	288	206	0.72	119	0.000018	0.03	0.4826	0.0057	11.141	0.140	0.4826	0.0057	0.941	2539	25	2532	7	0
23.1	851	44	0.05	157	0.001580	2.23	0.2105	0.0023	4.775	0.101	0.1645	0.0030	0.523	1232	12	2502	30	103
24.1	542	71	0.13	194	0.000266	0.38	0.4146	0.0046	9.359	0.114	0.4146	0.0046	0.911	2236	21	2495	8	12
25.1	399	115	0.29	161	0.000028	0.04	0.4708	0.0055	10.933	0.133	0.4708	0.0055	0.951	2487	24	2542	6	2
26.1	717	73	0.10	292	0.000043	0.06	0.4741	0.0051	10.661	0.119	0.4741	0.0051	0.966	2501	22	2488	5	-1
27.1	1799	15	0.01	417	0.000062	0.09	0.2697	0.0028	4.799	0.052	0.1290	0.0004	0.966	1539	14	2085	5	35
28.1	595	90	0.15	201	0.000234	0.33	0.3924	0.0043	8.531	0.102	0.1577	0.0007	0.919	2134	20	2431	8	14
29.1	239	159	0.66	103	0.000016	0.02	0.4992	0.0070	11.415	0.169	0.4992	0.0070	0.948	2610	30	2516	8	-4
30.1	160	80	0.50	64	0.000024	0.03	0.4676	0.0063	10.918	0.160	0.4676	0.0063	0.916	2473	28	2551	10	3
31.1	191	115	0.60	81	0.000038	0.05	0.4908	0.0061	11.640	0.157	0.4908	0.0061	0.925	2574	27	2577	9	0
31.2	875	52	0.06	267	0.000451	0.64	0.3527	0.0038	7.689	0.095	0.1581	0.0010	0.863	1947	18	2436	11	25
32.1	1978	49	0.02	189	0.003142	4.80	0.1060	0.0012	1.750	0.091	0.1197	0.0060	0.217	650	7	1952	90	200
33.1	262	55	0.21	106	0.000042	0.06	0.4701	0.0056	10.701	0.137	0.4701	0.0056	0.931	2484	25	2508	8	1
34.1	444	131	0.30	155	0.000184	0.26	0.4059	0.0046	9.253	0.115	0.4059	0.0046	0.904	2196	21	2511	9	14
35.1	209	137	0.66	79	0.000033	0.05	0.4423	0.0054	10.191	0.136	0.4423	0.0054	0.915	2361	24	2529	9	7
36.1	1831	35	0.02	227	0.002309	3.52	0.1390	0.0015	2.304	0.088	0.1202	0.0044	0.285	839	9	1960	66	134
37.1	92	109	1.18	38	0.000144	0.20	0.4845	0.0086	10.857	0.213	0.4845	0.0086	0.908	2547	37	2482	14	-3
38.1	76	30	0.39	39	-	<0.01	0.6014	0.0091	18.161	0.302	0.6014	0.0091	0.915	3036	37	2973	11	-2
39.1	306	45	0.15	120	0.000001	<0.01	0.4559	0.0053	10.374	0.128	0.4559	0.0053	0.939	2422	23	2508	7	4
40.1	158	85	0.54	66	0.000025	0.03	0.4877	0.0063	12.000	0.169	0.4877	0.0063	0.916	2561	27	2638	9	3
41.1	363	53	0.15	138	0.000074	0.10	0.4433	0.0051	10.086	0.122	0.4433	0.0051	0.946	2365	23	2508	7	6
42.1	224	194	0.87	80	0.000067	0.09	0.4169	0.0051	10.486	0.140	0.4169	0.0051	0.909	2246	23	2675	9	19
43.1	194	100	0.51	79	0.000122	0.17	0.4711	0.0060	11.089	0.154	0.4711	0.0060	0.916	2488	26	2565	9	3
23.2	405	227	0.56	173	0.000094	0.13	0.4974	0.0056	12.504	0.147	0.4974	0.0056	0.952	2603	24	2674	6	3
44.1	412	68	0.16	147	0.000221	0.31	0.4151	0.0046	9.377	0.114	0.4151	0.0046	0.917	2238	21	2496	8	12
45.1	373	235	0.63	143	0.000239	0.33	0.4455	0.0050	10.945	0.134	0.4455	0.0050	0.920	2375	22	2636	8	11
46.1	515	491	0.95	185	0.000328	0.46	0.4155	0.0046	9.637	0.118	0.4155	0.0046	0.902	2240	21	2540	9	13
47.1	293	117	0.40	127	0.000054	0.07	0.5036	0.0058	11.950	0.147	0.5036	0.0058	0.943	2629	25	2578	7	-2

Notes :  
 1. Uncertainties given at the one s level.  
 2. f206 %denotes the percentage of <sup>206</sup>Pb that is common Pb.  
 3. Correction for common Pb made using the measured <sup>204</sup>Pb/<sup>206</sup>Pb ratio.  
 4. For %Disc., 0%denotes a concordant analysis.

Table 6. Chemical composition of Wangary Gneiss and Carnot paragneisses. (La/Yb)<sub>N</sub> and (Gd/Yb)<sub>N</sub> are chondrite normalized ratios; chondrite REE abundances from Taylor and McLennan (1985); Eu/Eu\* = 2\*Eu<sub>N</sub>/(Sm<sub>N</sub> + Gd<sub>N</sub>).

Unit	Wangary Gneiss (Datum GDA 94 Z53)					Carnot Paragneiss			
Sample #	A2030-02	A2030-03	A2030-04	A2030-05	A2030-06	A2030-74	A2030-78	A2030-81	A2030-82
Eastings	535625	535525	535525	535625	535625	545358	545376	545376	545376
Northings	6188937	6187483	6187483	6188937	6188937	6151126	6151247	6151247	6151247
Location	Frenchmans					Shoal Point			
SiO <sub>2</sub>	54.20	64.7	70.9	68.3	64.8	49.7	47.5	49.7	57.4
TiO <sub>2</sub>	0.76	0.625	0.65	0.49	0.92	1.13	0.735	1.06	0.755
Al <sub>2</sub> O <sub>3</sub>	21.60	16.8	12.6	16.1	16	22	27.2	20.8	20.9
Fe <sub>2</sub> O <sub>3</sub>	9.21	6.61	5.42	4.2	6.12	11.9	10.3	14.4	8.27
MnO	0.10	0.07	0.04	0.03	0.05	0.12	0.12	0.22	0.07
MgO	3.81	2.86	2	1.82	2.17	5.8	5.47	5.13	4.11
CaO	0.48	0.9	1.37	0.99	2.54	1.39	2.17	2.23	1.44
Na <sub>2</sub> O	1.22	1.96	2.92	1.76	2.9	2.55	2.37	2.4	2.29
K <sub>2</sub> O	5.31	3.48	2.61	3.54	2.95	3.86	2.93	3.16	2.86
P <sub>2</sub> O <sub>5</sub>	0.05	0.03	0.06	0.04	0.04	<0.01	0.04	0.03	0.01
S	0.02	<0.01	0.04	<0.01	<0.01	0.27	0.06	<0.01	0.3
LOI	2.43	1.78	1.31	2.21	1.26	1.18	1.13	0.52	1.35
La	40.00	43.5	54	57	59	57	50	40.5	58
Ce	57.00	60	73	80	78	77	76	50	79
Pr	7.00	7.5	8.5	9.5	9.5	8.5	9	6	9.5
Nd	26.50	27	30.5	33.5	34.5	31.5	32	20.5	34.5
Sm	5.00	5	5.5	6.5	6	5.5	6	4.5	6
Eu	0.86	1.05	1	1.15	1.85	1.5	1.55	1.2	1.6
Gd	2.80	3	3.1	3.6	3.6	4.1	3.8	5	3.8
Tb	0.48	0.45	0.5	0.58	0.58	0.95	0.86	1.6	0.76
Dy	2.20	2	2.4	2.8	2.7	6.5	6.5	11.5	5
Ho	0.27	0.25	0.31	0.35	0.34	1.15	1.2	2.1	0.85
Er	0.70	0.6	0.8	0.85	0.95	3.5	3.8	6.5	2.7
Tm	0.10	0.05	0.1	0.1	0.15	0.5	0.5	0.9	0.35
Yb	0.55	0.5	0.75	0.75	0.85	3.6	3.3	6.5	2.5
Lu	0.09	0.08	0.12	0.11	0.12	0.49	0.4	0.82	0.34
(La/Yb) <sub>N</sub>	49.15	58.79	48.65	51.36	46.90	10.70	10.24	4.21	15.68
Eu/Eu*	0.64	0.77	0.68	0.66	1.13	0.93	0.93	0.77	0.96
(Gd/Yb) <sub>N</sub>	4.13	4.86	3.35	3.89	3.43	0.92	0.93	0.62	1.23
Y	7.00	7	8.5	9.5	10	34	35.5	63	27
Cr	220.00	210	160	90	100	310	280	270	200
V	180.00	120	100	70	100	250	190	200	160
Sc	20.00	15	10	10	15	30	25	35	20
Ni	62.00	58	28	25	30	130	90	88	115
Co	32.50	39	36	41.5	34.5	56	49	52	54
Cu	37.00	78	38	39.5	36	140	46	120	120
Zn	135.00	110	84	71	80	130	340	430	130
Cr/V	1.22	1.75	1.60	1.29	1.00	1.24	1.47	1.35	1.25
V/Ni	2.90	2.07	3.57	2.80	3.33	1.92	2.11	2.27	1.39
Ni/Co	1.91	1.49	0.78	0.60	0.87	2.32	1.84	1.69	2.13
Cs	14.00	8	8.5	3.6	4	0.5	0.5	0.4	0.3
Rb	250.00	130	125	150	120	51	67	125	49
Tl	2.10	1.2	1.2	1	1.1	0.6	0.9	1.1	0.5
Ba	350.00	350	155	390	440	700	370	600	600
Pb	15.50	23	24.5	31.5	23.5	13.5	28.5	62	14
Sr	160.00	110	240	115	250	85	130	125	160
Th	11.50	13.5	15.5	20	15	9	10	6.5	15
U	4.80	3.3	3	4.4	2.7	0.38	0.87	0.44	0.64
Zr	140.00	140	270	160	260	240	210	270	170
Hf	3.00	3	3	4	4	5	3	3	4
Nb	12.50	9.5	8	7.5	10	11.5	5	22	6
Mo	2.00	0.4	0.7	0.6	0.6	3.7	3.1	5.5	3.6
W	165.00	180	220	280	220	185	195	240	250
Bi	1.50	4.6	5.5	0.1	0.3	<0.1	<0.1	<0.1	<0.1
Zr/Hf	46.67	46.67	90.00	40.00	65.00	48.00	70.00	90.00	42.50
Th/U	2.40	4.09	5.17	4.55	5.56	23.68	11.49	14.77	23.44
La/Th	0.21	0.13	0.08	0.11	0.08	0.13	0.11	0.08	0.09
Au	3.00	2	2	2	2	2	2	3	2
Ag	0.30	0.2	0.3	0.2	0.3	0.3	0.2	0.5	0.2
As	115.00	31.5	26.5	1	<0.5	<0.5	<0.5	<0.5	<0.5
Be	3.50	3	4	3.5	2	<0.5	1	2	0.5
Ga	39.50	30.5	21	27.5	25	38	39	42.5	36
Pr	7.00	7.5	8.5	9.5	9.5	8.5	9	6	9.5

Table 7. Sm-Nd data from the Wangary Gneiss and Carnot paragneisses of the Sleaford Complex.

Unit	Nd	Sm	$^{143}\text{Nd}/^{144}\text{Nd}$	$^{147}\text{Sm}/^{144}\text{Nd}$	Strat (T)	age	$\epsilon_{\text{Nd}}(0)$	$\epsilon_{\text{Nd}}(T)$	$T_{\text{DM}}$
<b>Wangary Gneiss</b>									
A2030 2	31.93	5.75	0.511114±7	0.1088	2520 Ma		-29.72	-1.27	2961 Ma
A2030 3	23.84	4.54	0.511174±8	0.1150	2520 Ma		-28.56	-2.14	3057 Ma
A2030 6	42.19	7.33	0.51100±1	0.1050	2520 Ma		-31.95	-2.27	3017 Ma
<b>Carnot paragneiss</b>									
A2030 74	51.95	8.65	0.510839±1	0.1006	2520 Ma		-35.10	-4.02	3115 Ma
A2030 78	41.26	6.88	0.511007±9	0.1008	2520 Ma		-31.82	-0.77	2896 Ma
A2030 81	22.47	4.93	0.51136±1	0.1325	2520 Ma		-24.87	-4.10	3357 Ma
A2030 82	37.12	6.07	0.510979±1	0.0988	2520 Ma		-32.36	-0.68	2884 Ma

Errors on  $^{143}\text{Nd}/^{144}\text{Nd}$  measurements are within  $2\sigma$  (mean) and refer to the last significant figures.  $\epsilon_{\text{Nd}}$  values calculated with CHUR (Goldstein et al, 1984) and depleted mantle model ages ( $T_{\text{DM}}$ ) from Goldstein et al, 1984 depleted mantle model curve.

## Appendix

Geological note: Nd isotopic constraints on stratigraphic components within the Carnot Gneiss

### *1.1 Shoal Point East Data*

Carnot paragneisses were sampled from Shoal Pt East and Shoal Pt for geochemical and Sm-Nd isotopic analyses (Figure 15 b). Initial  $\epsilon_{Nd}$  signatures of Shoal Pt East metasedimentary rocks (Table 8) calculated at a rock formation age of 2520 Ma, are significantly more juvenile than the Carnot paragneiss samples from Shoal Pt (+5.5, +5.6 and + 0.11, compared to -0.7 to -4.0). In addition, the depleted mantle model ages of samples A2030 7 and 16 ranges from 2460 to 2470 Ma which is significantly younger (~ 400-700 Ma) than other Carnot paragneiss analyses. Sample A2030-14 of the Shoal Pt East metasedimentary rocks is more evolved than A2030 7 and 16 with  $\epsilon_{Nd}(2520\text{Ma})$  of +0.11 and a depleted mantle model age of 2860 Ma. When the initial  $\epsilon_{Nd}$  signatures of the Shoal Pt East metasedimentary rocks are recalculated at 1850 Ma, (the rock formation age for the rift related Hutchison Group metasedimentary rocks which unconformably overly late Archaean rocks on Eyre Peninsula, Daly et al., (1993)). Samples A2030 7 and 16 from the Shoal Point East granulites are comparable to Sm-Nd isotopic analyses of the Hutchison group (Table 9), where initial  $\epsilon_{Nd}$  signatures (-2.9 to -3.0 and -1.9 to -3.2) and depleted mantle model ages (2460-2470 Ma and 2460-2530 Ma) overlap.

It is known that pervasive deformation during the Kimban Orogeny (1740-1710 Ma), (Schwarz et al., 2002) has resulted in structural repetitions of Hutchison Group with Archaean basement to the west of Cape Carnot. At Coles Point (Figure 15), the Warrow Quartzite (Hutchison Group) unconformably overlies the Wangary Gneiss, and at Marble Range the Warrow Quartzite overlies Kiana Granite (Figure 15 and 17). It is conceivable that the extent of this repetition has not been fully evaluated and the metasedimentary rocks at Shoal Point East may represent previously unrecognized Hutchison Group.

In mineralogy and outcrop style, the Shoal Pt East metasedimentary rocks are virtually identical from the Carnot paragneisses, with typical granulite grade metapelitic assemblages of garnet + cordierite + plagioclase + biotite + sillimanite present in both units. REE analyses (Table 10) of the Shoal Pt East metasedimentary rocks are very similar to Hutchison Group metasediments (Figure 16). However, it is difficult to differentiate between the Carnot paragneisses and the Hutchison Group REE patterns. Consequently it is possible that current interpretations on the extent of the Carnot Gneisses are not correct, and for example, Carnot Gneisses at Cape Carnot may actually be a mixture of Archaean and Palaeoproterozoic (Hutchison Group) rocks. A comprehensive Sm-Nd isotopic study of the rocks along the Cape Carnot coastline could provide further insights into this validity of this theory.

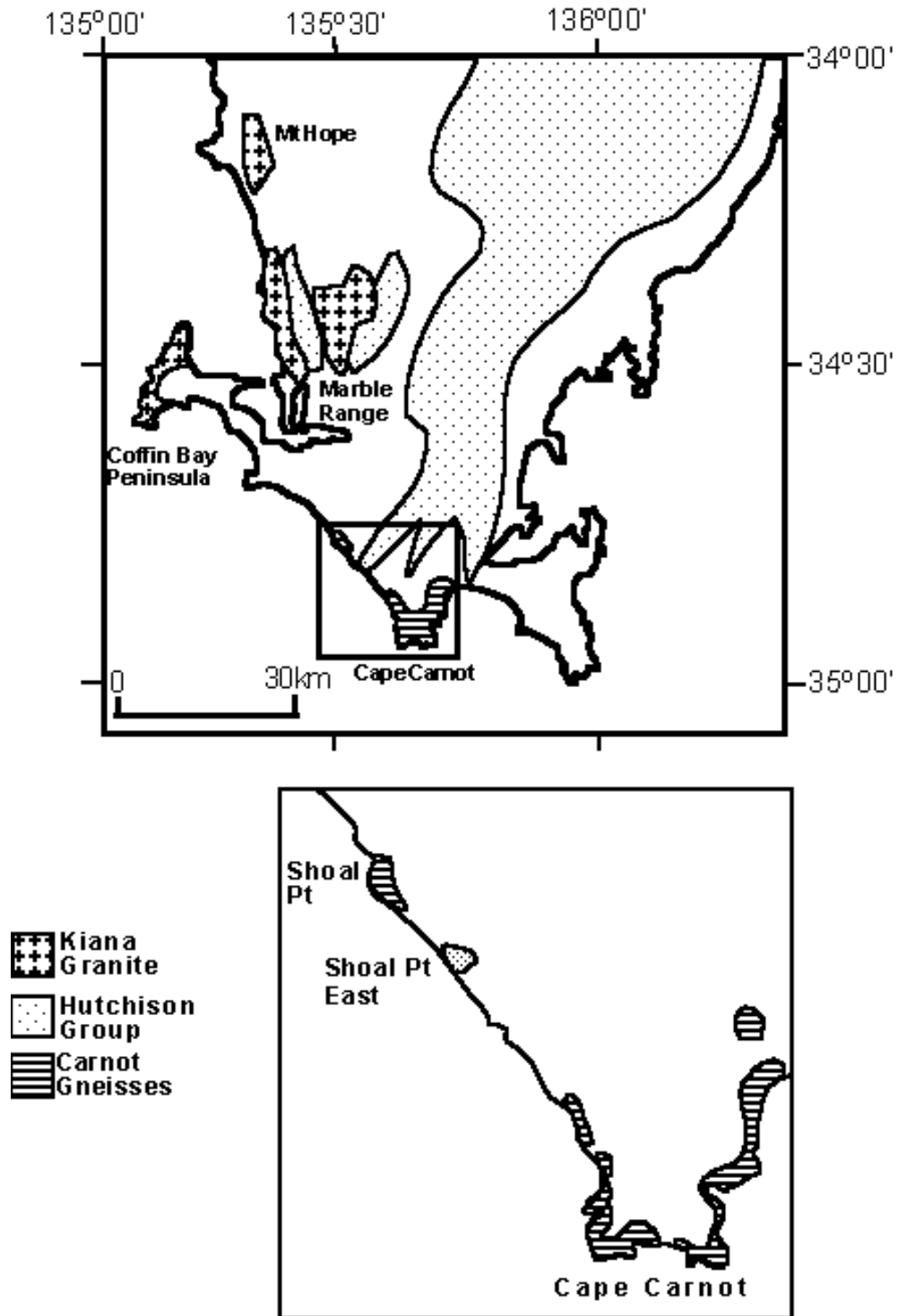


Figure 15. Map of known outcrop distribution of the Carnot Gneiss, Kiana Granite and Hutchison Group; inset shows distribution and Carnot Gneisses and outcrop location of Shoal Pt East metasedimentary rocks.

Table 8. Units A2030 7, 14 and 16 are mapped as Carnot Gneiss, however they have  $\epsilon_{Nd}$  which indicate a younger, Proterozoic cover sequence

Sample number	Nd	Sm	$^{143}Nd/^{144}Nd$	$^{147}Sm/^{144}Nd$	$\epsilon_{Nd}$ (2520 Ma)	$\epsilon_{Nd}$ (1850 Ma)	$T_{DM}$ (Ma)
A2030 7	43.37	7.17	0.511310±9	0.0999	+5.5	-3.0	2472 Ma
A2030 14	60.85	10.49	0.511109±9	0.1042	+0.1	-8.0	2819 Ma
A2030 16	58.31	9.53	0.511300±9	0.0988	+5.6	-2.9	2462 Ma

Errors on  $^{143}Nd/^{144}Nd$  measurements are within  $2\sigma$  (mean) and refer to the last significant figures.  $\epsilon_{Nd}$  vales calculated with CHUR (Goldstein et al, 1984) and depleted mantle model ages ( $T_{DM}$ ) from Goldstein et al, 1984 depleted mantle model curve

Table 9. Sm-Nd data from the various units of the Hutchison Group

Hutchison group	Nd	Sm	$^{143}Nd/^{144}Nd$	$^{147}Sm/^{144}Nd$	Strat age (T)	$\epsilon_{Nd}$ (T)	$T_{DM}$ (Ma)	Reference
Yadnarie schist	38.2	7.0	0.51150±6	0.111	1850	-1.9	2460	Simpson, 1994
Pelite	92.9	15.5	0.51131±3	0.101	1850	-3.2	2500	Schaefer, 1998
CGS	37.5	6.7	0.51140±3	0.108	1850	-3.1	2530	Turner et al., 1993
Yadnarie Schist	38.3	7.0	0.51150±6	0.1112	1850	-1.9	2460	Simpson, 1994
Cook Gap Schist	37.5	6.7	0.51140±3	0.1077	1850	-3.0	2520	Simpson, 1995

Errors on  $^{143}Nd/^{144}Nd$  measurements are within  $2\sigma$  (mean) and refer to the last significant figures.  $\epsilon_{Nd}$  vales calculated with CHUR (Goldstein et al, 1984) and depleted mantle model ages ( $T_{DM}$ ) from Goldstein et al, 1984 depleted mantle model curve

Ailsa Woodhouse, 2002.

Table 10. Geochemical Composition of Shoal Pt East, Hutchison Group samples. (La/Yb)<sub>N</sub> and (Gd/Yb)<sub>N</sub> are chondrite normalized ratios; chondrite REE abundances from Taylor and McLennan (1985);  $Eu/Eu^* = 2 * Eu_N / (Sm_N + Gd_N)$ .

Unit	Shoal Point East Hutchison Group					
Sample #	R5056780	R5056781	R5056782	R5056783	R5056784	R5056785
Eastings	548883	548883	548835	548835	548835	548835
Northings	6147774	6147774	6147807	6147807	6147807	6147807
Location	Shoal Point East					
SiO <sub>2</sub>	74.8	67	66.7	64.9	65.1	67.9
TiO <sub>2</sub>	0.75	0.715	0.935	1.09	1.01	0.98
Al <sub>2</sub> O <sub>3</sub>	10.9	14	14.9	15.4	15.9	14.4
Fe <sub>2</sub> O <sub>3</sub>	4.84	9.46	7.57	8.19	8.24	5.35
MnO	0.12	0.62	0.12	0.13	0.16	0.14
MgO	1.34	2.47	2.51	2.89	2.65	1.26
CaO	1.08	1.43	1.01	1.09	1.3	2.74
Na <sub>2</sub> O	1.39	1.49	1.28	1.23	1.55	2.57
K <sub>2</sub> O	3.95	3.49	4.38	3.8	3.75	2.95
P <sub>2</sub> O <sub>5</sub>	0.05	0.05	0.04	0.03	0.04	0.13
S	<0.01	<0.01	0.02	0.01	0.02	0.05
LOI	0.35	0.1	0.73	1.04	0.48	0.82
La	79	105	100	96	100	700
Ce	110	150	140	130	140	950
Pr	13	17	16.5	15.5	16	99
Nd	45.5	61	59	55	56	320
Sm	7.5	11.5	10.5	9.5	10	42.5
Eu	1.7	1.65	1.95	1.7	1.9	3.2
Gd	4.6	7.5	6.5	6	6	21
Tb	0.84	1.6	1.25	1.2	1.3	2.7
Dy	5.5	10	7	6.5	8.5	11
Ho	0.9	1.65	1.05	0.92	1.4	1.4
Er	2.9	5.5	3.1	2.4	4.4	3.8
Tm	0.4	0.7	0.4	0.3	0.6	0.4
Yb	3	5	2.8	1.95	4.3	2.7
Lu	0.41	0.66	0.39	0.28	0.59	0.38
(La/Yb) <sub>N</sub>	17.79	14.19	24.13	33.27	15.72	175.19
Eu/Eu*	0.82	0.51	0.67	0.64	0.69	0.29
(Gd/Yb) <sub>N</sub>	1.24	1.22	1.88	2.49	1.13	6.30
Y	27.5	51	32.5	28	43.5	42.5
Cr	100	80	100	130	120	30
V	80	90	120	140	130	60
Sc	10	15	15	15	15	10
Ni	20	18	39	40	42	9
Co	53	53	52	44.5	47	38.5
Cu	7.5	15	23	21.5	31	30
Zn	69	105	110	120	110	59
Cr/V	1.25	0.89	0.83	0.93	0.92	0.50
V/Ni	4.00	5.00	3.08	3.50	3.10	6.67
Ni/Co	0.38	0.34	0.75	0.90	0.89	0.23
Cs	0.9	0.9	1.7	2	1.6	1
Rb	110	99	140	100	150	59
Tl	0.7	0.6	0.8	0.8	0.7	0.5
Ba	600	600	750	450	850	430
Pb	34	24.5	47.5	39.5	44.5	44.5
Sr	130	120	140	105	155	160
Th	24	34	29.5	28.5	27.5	190
U	1.5	2.9	1.55	1.4	1.6	7
Zr	390	280	340	370	340	1050
Hf	7	4	11	10	9	20
Nb	10	10	13.5	16	16	21
Mo	0.2	0.6	0.2	0.2	0.2	0.2
W	410	420	350	250	280	300
Bi	<0.1	<0.1	<0.1	<0.1	<0.1	<0.1
Zr/Hf	55.71	70.00	30.91	37.00	37.78	52.50
Th/U	16.00	11.72	19.03	20.36	17.19	27.14
La/Th	0.01	0.00	0.02	0.04	0.02	0.00
Au	2	<1	<1	<1	3	<1
Ag	0.4	0.3	0.9	0.5	0.4	0.7
As	<0.5	<0.5	<0.5	<0.5	<0.5	<0.5
Be	<0.5	1	3.5	5	7.5	<0.5
Ga	17	21	27	30	29.5	25.5
Pr	13	17	16.5	15.5	16	99

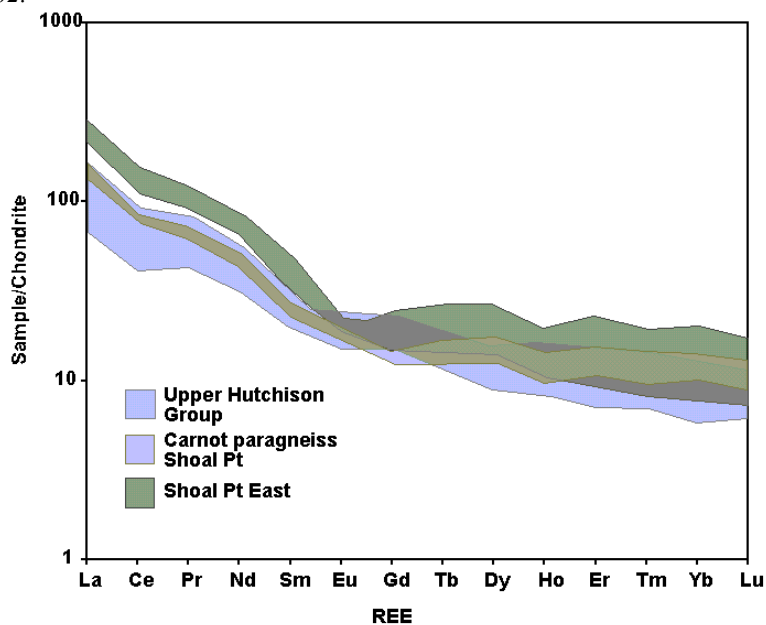


Figure 16. Chondrite normalized REE diagram of the Hutchison Group (M.E.R. data. in prep), Shoal Pt East metasedimentary rocks and Carnot paragneisses.

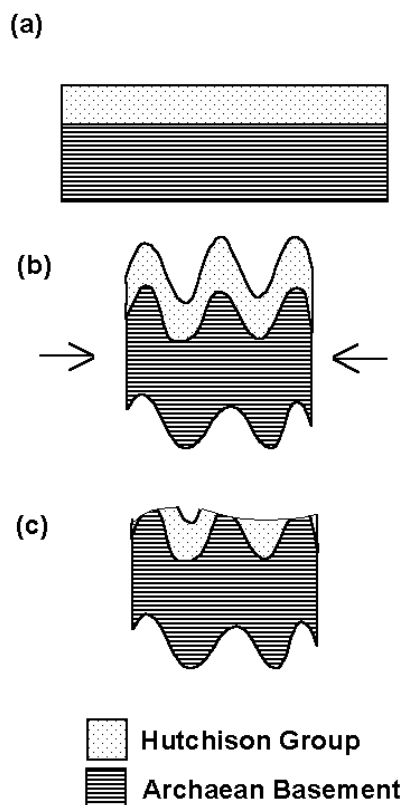


Figure 17. Schematic diagram of structural repetitions of the Hutchison Group metasediments with Archaean Basement; (a) Hutchison group is deposited on Archaean basement; (b) folding during the Kimban Orogeny 1740-1710 Ma (Schwarz et al., 2002); (c) erosion results in structural repetitions of Hutchison Group with Archaean basement.